Chapter 6

WESTERN PACIFIC AND MARGINAL SEA PROCESSES

TANGDONG QU

International Pacific Research Center, SOEST, University of Hawaii, Honolulu, USA

TOMOKI TOZUKA

Department of Earth and Planetary Science, Graduate School of Science, The University of Tokyo, Tokyo, Japan

SHINICHIRO KIDA

Application Laboratory, Japan Agency for Marine–Earth Science and Technology, Yokohama, Japan

XINYU GUO

Center for Marine Environmental Studies, Ehime University, Matsuyama, Japan

YASUMASA MIYAZAWA

Application Laboratory, Japan Agency for Marine–Earth Science and Technology, Yokohama, Japan

QINYU LIU

Physical Oceanography Laboratory, Ocean University of China, Qingdao, China

This article focuses on the physical and dynamical processes of the marginal seas of the Western Pacific. The nature of the circulation regimes and their interconnectivity are discussed in detail, with emphasis on individual basins. In addition to the Kuroshio and its variability in the North Pacific, the circulation regimes in the South China Sea and Indonesian Seas are presented for an overall view of the circulation system. These circulations play important roles in regional ocean dynamics and global climate variations such as the El Niño/Southern Oscillation.

1. Western Pacific Circulation

The western tropical Pacific is considered very important for various reasons. First, the warm pool in this region plays a key role in the El Niño/Southern Oscillation (ENSO; Chang *et al.* 2006), which influences global climate through atmospheric teleconnections. Also, it is located in the upstream of the Indonesian Throughflow (Gordon and Kamenkovich 2010), a key component of the global thermohaline circulation (Gordon 1986; Broecker 1991) which controls the global climate (Santoso *et al.* 2011). This is why the Northwestern

Indo-Pacific Climate Variability and Predictability
edited by Swadhin Kumar Behera and Toshio Yamagata

Pacific Ocean Circulation and Climate Experiment (NPOCE) was recently introduced to conduct collaborative research including field experiments in this area (Wang and Hu 2010). In this section, we review major current systems, including the North Equatorial Current (NEC), Kuroshio/Luzon Undercurrent (LUC), Mindanao Current (MC)/Mindanao Undercurrent (MUC), and New Guinea Coastal Current (NGCC)/New Guinea Coastal Undercurrent (NGCUC), and an oceanic phenomenon called the Mindanao Dome. The surface current systems and the dome are shown in Fig. 1. We note that the focus is more on the circulation in the Northern Hemisphere. In addition, the importance of the western Pacific in ENSO

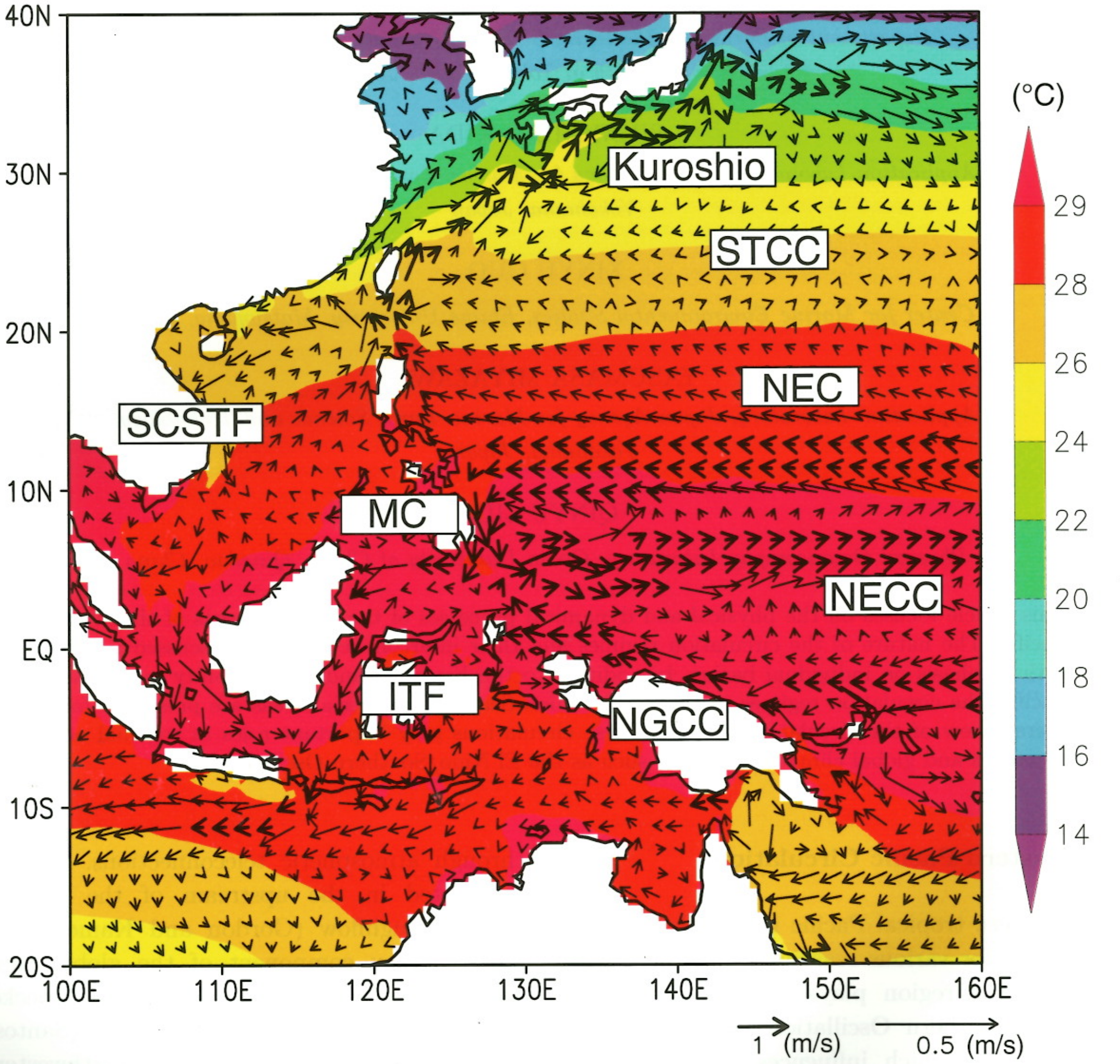

Fig. 1. Annual mean sea surface temperature and surface current averaged over the upper 50 m based on the Simple Ocean Data Assimilation (SODA). Currents larger (smaller) than 0.25 m/s are drawn with thick (thin) vectors. Also drawn are major current systems in the western Pacific. STCC — Subtropical Countercurrent; NEC — North Equatorial Current; SCSTF — South China Sea Throughflow; MC — Mindanao Current, NECC — North Equatorial Countercurrent; ITF — Indonesian Throughflow; and NGCC — New Guinea Coastal Current.

is briefly reviewed. We start with the western tropical Pacific, because the South China Sea throughflow (Sec. 2), the Indonesian Throughflow (Sec. 3), and the Kuroshio in the East China Sea (Sec. 4) originate from here.

1.1. *North Equatorial Current and Its Bifurcation Latitude*

When the NEC hits the Philippine coast, it bifurcates to the northward flowing Kuroshio discussed in Sec. 1.2 and the southward-flowing MC discussed in Sec. 1.3 (Toole *et al.* 1990). According to Qu *et al.* (1998), the mean transport of the NEC is 41 Sv, of which 14 Sv becomes the Kuroshio and 27 Sv becomes the MC. Since the variability in bifurcation of the NEC influences the heat budget of the western Pacific warm pool (Tozuka *et al.* 2007a; Ishida *et al.* 2008), it is considered to play an important role in climate (Qiu and Chen 2010).

The mean NEC bifurcation latitude (NBL) was estimated to be 13.3°N by Qu and Lukas (2003) using historical temperature and salinity data, 13.4°N by Wang and Hu (2006) using sea surface height observation, and 14.7°N by Chen and Wu (2011) using the 1.5-layer nonlinear reduced gravity model. The NBL is depth-dependent, and on the annual mean, it shifts from 13.3°N near the surface to north of 20°N at about 1000 m depth (Qu and Lukas 2003).

The NBL undergoes seasonal variations; the NEC bifurcates at its southernmost latitude (14.8°N estimated by Qu and Lukas 2003, and 12.9°N estimated by Wang and Hu 2006) in June–July and its northernmost latitude in November–December (17.2°N estimated by Qu and Lukas 2003, and 14.1°N estimated by Wang and Hu 2006).

Recently, several studies have focused on the dynamics of seasonal variations in the NBL. Using the 1.5-layer nonlinear reduced gravity model and first-mode baroclinic Rossby wave model, Chen and Wu (2011) showed that the seasonal meridional migration of the NBL is amplified by the coastal Kelvin waves generated by the extratropical winds with minor influence on the phase; about 50% of the total migration is accounted for by the coastal Kelvin waves excited north of 25°N. Also, the amplitude of the seasonal variation in the NBL increases from about 0.3° to 1.5° as the oceanic stratification intensifies, and the phase speed of the first baroclinic Rossby wave increases from $0.1\,\mathrm{m\,s^{-1}}$ to $0.25\,\mathrm{m\,s^{-1}}$ around the bifurcation latitude. This is because if the Rossby waves propagate faster, less cancelation with the wind forcing to the west occurs. Local seasonal wind forcing is most important in the phase of seasonal variation in the NBL, and Qiu and Chen (2010) showed that the surface wind forcing that is most relevant to the bifurcation latitude is located in 12°N–14°N and 140°E–170°E.

During El Niño (La Niña) years, the NEC tends to bifurcate at higher (lower) latitudes (Qiu and Lukas 1996; Kim *et al.* 2004; Wang and Hu 2006). However, the exact bifurcation latitude depends on the surface wind forcing over the western tropical North Pacific containing variability that is not linked with ENSO (Qiu and Chen 2010). For monitoring of the interannual variation, the sea surface height anomaly in the 12°N–14°N, 127°E–130°E box, which is located to the east of the mean NBL, may be useful, since this proxy explains 92% of the observed variance (Qiu and Chen 2010). The interannual variation of the NBL also has a profound effect on the larval transport of the Japanese eel (Kim *et al.* 2007), whose spawning area is located in the NEC to the west of the Mariana Islands (Tsukamoto 1992). Much less larvae were transported to the north with Kuroshio during El Niño years, because the NEC tends to bifurcate further to the north and less larvae can enter the northward flow.

1.2. *Kuroshio/Luzon Undercurrent*

The Kuroshio flows northward after the NEC bifurcates at the Philippine coast (Rudnick *et al.*

2011). It undergoes both seasonal and interannual variations. Its transport is at its seasonal maximum (minimum) around March (October) (Yaremchuk and Qu 2004), whereas the interannual variation is closely linked with the interannual variation of the NBL.

The Kuroshio transport is closely linked with the flow at the Luzon Strait (Sheremet 2001). The transport into the South China Sea (SCS) through the Luzon Strait decreases (increases) when the Kuroshio is stronger (weaker) (Qu *et al.* 2004). More details on the Luzon Strait throughflow and the Kuroshio in the downstream in the East China Sea and along the southern coast of Japan are given in Secs. 2 and 4, respectively.

Beneath the Kuroshio, there exists an equatorward-flowing current called the LUC (Qu *et al.* 1997). Although it varies considerably, it is considered to be a permanent feature with a mean geostrophic volume transport of 3.6 Sv and a width of about 50 km. Regarding its origin, Qu *et al.* (1997) suggested that about 28% of its transport is composed of the North Pacific Intermediate Water, whereas Gao *et al.* (2012) showed that 41% of the water can be traced back to the winter mixed layer in the Kuroshio Extension region, where the subtropical mode water is formed. The formation and variation of the LUC were suggested to be linked with the bifurcation dynamics (Qu *et al.* 1997), but its mechanism has not been examined quantitatively.

1.3. *Mindanao Current/Mindanao Undercurrent*

The MC is a low-latitude western boundary current that flows equatorward after the NEC bifurcates at the Philippine coast (Lukas *et al.* 1996). A portion of it directly flows into the North Equatorial Countercurrent (NECC), but others flow into the Celebes Sea and retroflect eastward to join the NECC or flow southward through the Makassar Strait as the Indonesian Throughflow (Susanto and Gordon 2005). The Indonesian Throughflow will be discussed in Sec. 3.

Underneath the MC, the MUC was first discovered by Hu and Cui (1989) based on conductivity–temperature–depth (CTD) observations during the Tropical Ocean and Global Atmosphere (TOGA) program and then observed by ADCP during the Western Equatorial Pacific Ocean Circulation Study (WEPOCS) (Lukas *et al.* 1991). Although it is highly variable, both observations and simulations suggest the existence of multiple cores of the MUC (Hu and Cui 1989; Qu *et al.* 2012). However, we note that more long-term observations with high horizontal resolution are necessary to validate the existence of multiple cores. Also, the relation between the MUC and the LUC has not been investigated.

The variability has a dominant timescale of 25–100 days, in which subthermocline eddies may play a role (Firing *et al.* 2005), but annual and semiannual signals also exist (Kashino *et al.* 2005; Qu *et al.* 2008). On the interannual timescale, a strong, intermittent quasi-biennial signal was observed by sea-level data (Lukas 1988). Also, the interannual variations show some correspondence with ENSO both in observations (Kashino *et al.* 2009, 2011) and in numerical models (Kim *et al.* 2004), possibly due to the meridional migration of the NBL (Kim *et al.* 2004). However, the correlation with the Southern Oscillation Index is model-dependent (Kim *et al.* 2004; Qu *et al.* 2012) and requires further studies.

To understand their mechanisms, Qu *et al.* (2012) have calculated the mean momentum balance using outputs from the high-resolution OGCM. Since the Coriolis force and pressure gradient force were dominant, they suggested that the MC and MUC are approximately a geostrophic flow. However, as much as 50% of the inshore velocity core of the MUC was suggested to be explained by ageostrophic dynamics. Eddy-induced momentum flux made the most dominant contribution to the ageostrophic component. On the other hand, about 70% of the offshore velocity core of the MUC was in geostrophic balance.

1.4. *Mindanao Dome*

The Mindanao Dome is a thermocline dome associated with the NEC to the north, the MC to the west, and the NECC to the south. Its center is located around 130°E, 7°N and it is often associated with a cold eddy called the Mindanao Eddy. Based on OGCM experiments, Masumoto and Yamagata (1991) showed that the local Ekman upwelling is important for its development in boreal winter, and the downwelling Rossby waves excited in the same season by the northeasterly trade winds play an important role in its seasonal decay. Tozuka *et al.* (2002) further demonstrated that the downwelling Rossby waves originate from the eastern tropical Pacific as a part of annual ENSO (Tozuka and Yamagata 2003; Tozuka *et al.* 2005). The annual ENSO consists of the seasonal air–sea interaction in the eastern tropical Pacific with an east–west see-saw in the atmospheric pressure anomaly, and the off-equatorial Rossby waves are generated by the zonal wind anomalies associated with the air–sea interaction in the eastern tropical Pacific. The above mechanism is also supported by a coupled general circulation model (Suzuki *et al.* 2005). More recently, Kashino *et al.* (2011) used observation data from the Triangle Trans-Ocean Buoy Network (TRITON) buoys and Argo floats, and pointed out that the contribution of local and remote forcing is dependent on latitude. The local wind plays the dominant role in the annual variability at 5°N, but Rossby waves originating west of 150°W are more important at 8°N. In addition to the dominant annual harmonic, there exists a semiannual signal whose amplitude is 40–70% of that of the annual harmonic (Qu *et al.* 2008; Kashino *et al.* 2011).

Regarding its interannual variations, Tozuka *et al.* (2002) showed that modulations in both local Ekman upwelling and remotely forced downwelling Rossby waves linked with ENSO make important contributions. This was supported by recent observations by Kashino *et al.* (2011). During the 2002/03 and 2006/07 El Niño events, the Mindanao Dome became stronger, while it was less developed between these two El Niño events. Ekman downwelling anomalies that appeared east of 150°E from 2005 to 2006 are considered to play a role in the anomalous weakening of the dome.

1.5. *New Guinea Coastal Current/New Guinea Coastal Undercurrent*

The NGCC and NGCUC are the low-latitude western boundary currents in the tropical South Pacific. Although the NGCUC flows equatorward throughout the year, the surface NGCC reverses its direction in association with the monsoon winds and flows equatorward (poleward) during austral winter (summer). The NGCUC provides the source water of the Equatorial Undercurrent (Lindstrom *et al.* 1987). Their interannual variations are closely related to ENSO. Ueki *et al.* (2003) observed that the NGCC did not reverse its direction in austral summer and the NGCUC intensified in austral winter during the 1997/98 El Niño. These currents also vary intraseasonally, owing to intrinsic oceanic variability related to the New Guinea Eddy, but because of low coherence their link with the atmospheric intraseasonal variability is considered to be weak (Kashino *et al.* 2007).

1.6. *Subtropical Countercurrent*

The Subtropical Countercurrent (STCC) is a narrow eastward jet in the upper layer of the Northwest Pacific (20°N-30°N) (Yoshida and Kidokoro 1967; Uda and Hasunuma 1969) and is accompanied by a subsurface temperature and density front called the subtropical front (STF), suggesting a thermal wind relation between the STCC and the STF (Uda and Hasunuma 1969; White *et al.* 1978; Kobashi *et al.* 2006; Yamanaka *et al.* 2008). According to the hydrographic observation analysis of Kobashi *et al.* (2006), the STCC originates in the western Pacific around 20°N, flows against the northeast trade winds and stretches northeastward to north of Hawaii. Furthermore, the STCC maintains a stronger sea surface temperature (SST) front during winter and spring. The SST front also anchors a meridional maximum in column-integrated water vapor, leading to a deep structure in the atmospheric response during spring (Kobashi *et al.* 2008).

The subtropical mode water is shown to play an important role in the formation and maintenance of the STCC and STF by theoretical (Kubokawa 1997, 1999), simulation (Kubokawa and Inui 1999; Yamanaka *et al.* 2008), and observational (Kobashi *et al.* 2006) studies, because it appears as a minimum in the vertical gradient of temperature and density in the upper thermocline (i.e. a thermostad or pycnostad) (Kubokawa 1999; Xie *et al.* 2000). Using a 300-year control run simulation from the Geophysical Fluid Dynamics Laboratory (GFDL) coupled model CM2.1, Xie *et al.* (2011) showed that on decadal timescales the dominant mode of natural variability for sea surface height (SSH) in the central subtropical gyre (170°E–130°W, 15°N–35°N) is characterized by the strengthening and weakening of the STCC due to variations in mode water ventilation, which they called the STCC mode. The response of the STCC and its variability to global warming is examined in a state-of-the-art coupled model that is forced by increasing greenhouse gas concentrations (Xu *et al.* 2012a). As a response to increasing greenhouse gas, the subduction rate is reduced, the sea surface density in the Kuroshio Oyashio Extension (KOE) decreases, and the mode water forms on lighter isopycnals with reduced thickness. Advected southward, the weakened mode water formation results in deceleration of the STCC and the reduced decadal variability in the mode water formation leads to that in the STCC (Xu *et al.* 2012a). In 17 Coupled Model Intercomparison Project Phase 5 (CMIP5) model simulations, the STCC is anchored by the mode water to the north in the central North Pacific. For the present climate simulation, the STCC tends to be stronger in the models than in observations, because of the overestimated mode water in the models. Under global warming, the STCC becomes weaker because of the reduced formation of mode water (Xu *et al.* 2012b). The natural mode of decadal variability in the STCC can be excited by global warming, resulting in banded structures in the SST (Xu *et al.* 2012b).

Based on the altimetry data, Qiu (1999) detected that the eddy kinetic energy of the STCC was larger than any other regions in the western Pacific, except for the Kuroshio Extension, and showed a clear seasonal cycle. Compared to the eastward-flowing Hawaiian Lee Countercurrent (HLCC), baroclinic instability in the STCC is more remarkable, because of the difference in stratification in the STCC (Liu and Li 2007). Based on satellite observations (Chow and Liu 2012), eddies in the STCC area are generally characterized by a main period of about 100 days and a wavelength of about 600–800 km. Those eddies meet with the SST front and induce robust heat advection, which adjusts the SST spatial distribution to form the tonguelike pattern of warm and cold SST, and subsequently the adjusted SST influences surface wind speed on weather timescales (Chow and Liu 2012).

1.7. *The Western Pacific's Role in ENSO*

Since its heat content increases prior to an occurrence of El Niño (Wyrtki 1985), the western tropical Pacific is known to play a crucial role in the turnabout of ENSO (Chang *et al.* 2006). Recently, other features in the western Pacific have also been suggested to make an important contribution. First, westerly wind bursts (WWBs; Luther *et al.* 1983; Harrison and Vecchi 1997) in the western equatorial Pacific are considered to play a key role in the triggering of ENSO events by generating eastward-propagating downwelling Kelvin waves (McPhaden *et al.* 1988). According to Yu *et al.* (2003) and Eisenman *et al.* (2005), these WWBs are modulated by SST anomalies associated with ENSO. Barrier layers between the base of the mixed layer and the top of the thermocline are commonly observed in the western tropical Pacific (Lukas and Lindstrom 1991; Sprintall and Tomczak 1992; Delcroix and McPhaden 2002), but during some WWB events during La Niña, a thick barrier layer is formed as a result of enhanced rainfall and equatorward transport of fresh water from the Northern Hemisphere (Cronin and McPhaden 2002). The reduced entrainment of subsurface cold water caused by the thick barrier layer may contribute to the heat buildup in the western Pacific and the turnabout of ENSO (Maes *et al.* 2005).

Weisberg and Wang (1997) proposed the western Pacific oscillator paradigm. During a warm event, off-equatorial upwelling Rossby waves are generated by the equatorial westerly wind stress anomalies in the central Pacific. As they reach the western tropical Pacific, they shoal the thermocline depth and cause negative SST anomalies. In response, anomalous anticyclones are generated in the atmosphere and induce easterly wind stress anomalies in the far western equatorial Pacific. This forces upwelling equatorial Kelvin waves that contribute to the decaying of the warm event. From satellite observations (Boulanger *et al.* 2003) and OGCM results (Yuan *et al.* 2004), it was shown that the western Pacific oscillator was at work during the 1997/98 El Niño event. In contrast to the delayed oscillator paradigm (Suarez and Schopf 1988; Battisti and Hirst 1989), this does not require reflection of downwelling Rossby waves at the western boundary. The delayed oscillator paradigm proposes that off-equatorial upwelling (downwelling) Rossby waves forced by westerly (easterly) wind stress anomalies in the central Pacific reflect at the western boundary and propagate eastward as upwelling (downwelling) Kelvin waves to terminate El Niño (La Niña) and initiate La Niña (El Niño). Spall and Pedlosky (2005) recently quantified that 37% of the incident flux is reflected at the western boundary for a wind event of two-year duration with a meridional decay scale of 700 km. The above two paradigms are discussed in the framework of a "unified oscillator model" (Wang 2001).

Recently, a new mechanism regarding the turnabout of ENSO has been proposed. Hasegawa *et al.* (2009, 2010) suggested that coastal upwelling along the northern coast of Papua New Guinea generates negative SST anomalies there and a positive zonal SST gradient in the western Pacific. This may enhance the westerly wind stress anomalies that trigger El Niño events. Also, the southward shift of the westerly wind stress anomalies associated with the wind–evaporation–SST feedback induces easterly wind stress anomalies in the far western equatorial Pacific and may contribute to the decay of El Niño (Ueki 2011).

1.8. *Outstanding Issues*

Although understanding of the western Pacific circulation has advanced greatly over the past few decades, there are many issues that remain to be solved. First, there are many results based on modeling, such as the mechanism of interannual variations in the Mindanao Dome, that need to be validated by observations. Also, interannual variations in the bifurcation latitudes of the NEC are partly explained by ENSO, but other factors influencing the variations need to be clarified for both climatic and ecological reasons. Regarding the undercurrent systems, the relation between the MUC and the LUC needs to be investigated in the future. The detailed structure of the MUC, including the possible existence of multiple cores, need to be examined through dense observations. Finally, although

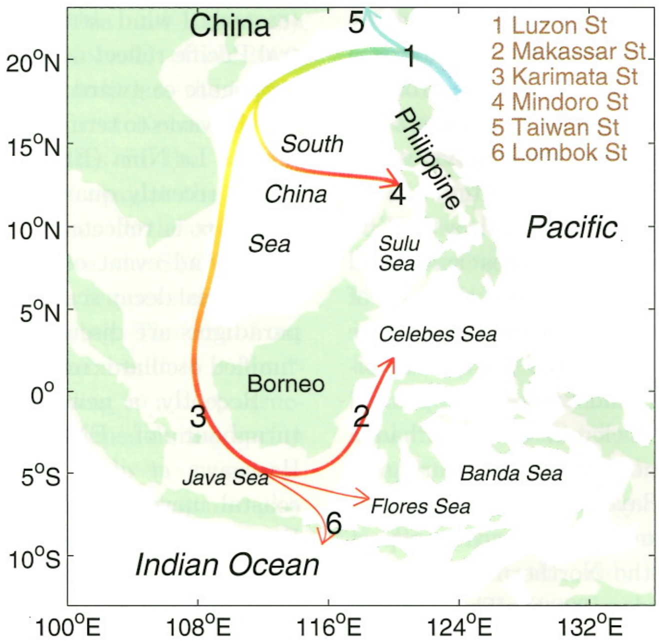

Fig. 2. A Schematic diagram of the South China Sea throughflow (after Qu *et al.*, 2006a). Water entering the South China Sea through the Luzon Strait is lower in temperature (blue) and higher in salinity (blue) than water leaving it through the Karimata, Mindoro, and Taiwan Straits.

the importance of the western Pacific in ENSO has long been recognized, its realistic reproduction in coupled models is not satisfactory at the moment and the new mechanisms operating in the western Pacific proposed by Hasegawa *et al.* (2009, 2010) and Ueki (2011) need to be further tested with a coupled model.

2. South China Sea Circulation and Throughflow

The South China Sea (SCS) is the largest marginal sea in the southeastern Asian waters, covering a surface area greater than one-third of the continental United States. It connects in the south with the Sulu and Java Seas mainly through the Mindoro Strait (~200 m) and Karimata Strait (<50 m), and in the north with the East China Sea and the Pacific Ocean through the Taiwan Strait (<100 m) and Luzon Strait (>2000 m), with a maximum water depth exceeding 5000 m in the central part of the basin (Fig. 2). Linking the Pacific and Indian Oceans, the SCS has been an important sea lane for over a thousand years. It formed part of the oceanic "Silk Road" which connected ancient China with the rest of the world. Today half a billion people live along the coast of the SCS, and with its fisheries and other natural resources the region has become one of the world's economic powerhouses.

On the basin average, the SCS receives heat from the atmosphere at a rate ranging from 20 to 50 $\mathrm{W\,m^{-2}}$ (Figs. 3a, b). Recent OAFlux data (Yu and Weller 2007) favor a mean value around the higher end of this range, 49 $\mathrm{W\,m^{-2}}$, which is nearly twice as high as the estimate (23 $\mathrm{W\,m^{-2}}$) from the Comprehensive Ocean–Atmosphere Data Set (Oberhuber 1988). With a surface area of about $3.5 \times 10^{12}\,\mathrm{m^2}$, these estimates imply a net heat gain of up to 0.1–0.2 PW (1 PW $= 10^{15}$ W) over the entire SCS basin. This heat gain from the atmosphere makes the SCS part of the tropical eastern Indian Ocean and

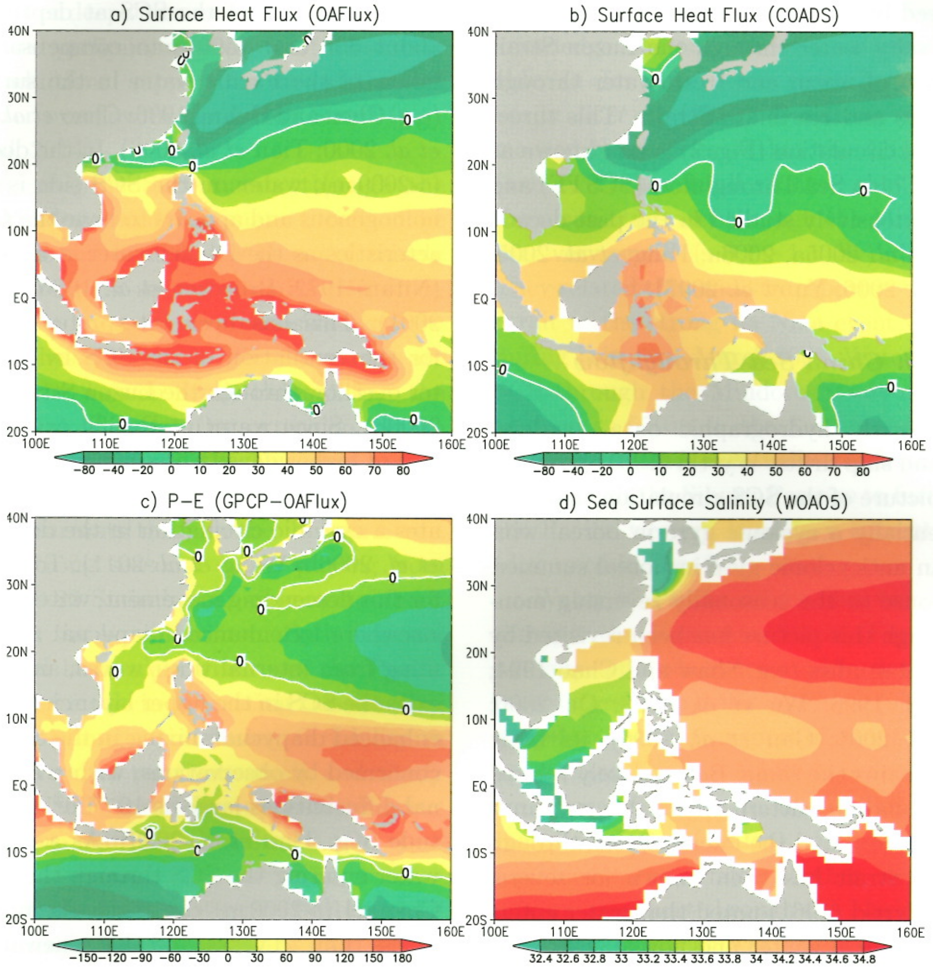

Fig. 3. Mean surface heat flux from (a) OAFlux (Yu and Weller 2007), (b) mean surface heat flux COADS (Oberhuber 1988), mean precipitation minus evaporation (P–E) from OAFlux and GPCP (Yu and Weller 2007; Adler *et al.* 2003), and (d) mean sea surface salinity from WOA05. The units are $\mathrm{W\,m^{-2}}$ in (a) and (b), $\mathrm{cm\,yr^{-1}}$ in (c), and psu in (d).

western Pacific warm pool, where SST changes are of particular importance to the world's climate (e.g. Wang *et al.* 2009; Yamagata *et al.* 2015; Masumoto *et al.* 2015).

Examination of the Climate Prediction Center Merged Analysis of Precipitation (CMAP; Xie and Arkin 1997) and the Global Precipitation Climatology Project (GPCP; e.g. Adler *et al.* 2003) precipitation data shows that the SCS is also a recipient of heavy rainfall, with an annual mean value of 0.2–0.3 Sv ($1\ \mathrm{Sv} = 1 \times 10^6\ \mathrm{m^3\,s^{-1}}$) over the entire basin. Preliminary analysis of OAFlux evaporation and CPGP precipitation data indicates that precipitation in the SCS exceeds evaporation (P–E) by at least 0.1 Sv (Fig. 3c), resulting in the freshest sea surface in the region (Fig. 3d). The contrast of sea surface salinity (SSS) between the SCS and its adjacent waters is believed to play a critical role in forcing the SCS circulation and modulating the Indonesian throughflow (discussed below).

The SCS is a semiclosed basin below about 200 m. On the long-term average, the heat and freshwater gain from the atmosphere can only be balanced by ocean advection, with inflow of cold and salty water through the Luzon Strait and outflow of warm and fresh water through the Mindoro and Karimata Straits. This three-dimensional circulation (Fig. 2) is now known as the South China Sea Throughflow (SCSTF) and has been extensively studied in the past decade (e.g. Qu *et al.* 2005a, 2006a; Fang *et al.* 2005; Wang *et al.* 2006; Yu *et al.* 2007).

2.1. *South China Sea Throughflow*

Based on early hydrographic data, sea-level records, and ship drifts, Wyrtki (1961) provided the first picture of the SCS circulation that contains essentially a cyclonic gyre in boreal winter and an anticyclonic gyre in boreal summer, as a response to the seasonally reversing monsoon. Though this picture has been revisited by many recent studies (e.g. Shaw and Chao 1994; Chao *et al.* 1996; Wu *et al.* 1998; Qu 2000; Fang *et al.* 2005; Gan *et al.* 2006), its basic pattern remains the same. Being closely related to this circulation pattern, the water exchange between the SCS and the Pacific Ocean through the Luzon Strait has been known for several decades. Wyrtki (1961) noted that water enters the SCS in boreal winter and flows back to the Pacific in boreal summer. This is true, however, only for the surface layer, where ocean circulation is predominantly forced by monsoonal winds. In the depth range of the thermocline (say, around 100 m), later observations revealed the existence of a Kuroshio branch toward the SCS in both boreal winter and summer (e.g. Qiu *et al.* 1984; Guo 1985), and the intrusion of the North Pacific Tropical Water seems to occur all year round (e.g. Shaw, 1989, 1991; Qu *et al.* 2000), presumably as a result of the westward pressure gradient along the continental slope south of China (e.g. Qu 2000; Hsueh and Zhong 2004).

The flow in the Luzon Strait changes its direction in the intermediate layer. Both observations and numerical models have shown that water flows out of the SCS at depths between about 500 and 1500 m to compensate for the inflow of the Pacific water in the surface layer (e.g. Chen and Huang 1996; Chao *et al.* 1996; Qu *et al.* 2000; Tian *et al.* 2006). In the deeper layer (>2000 m), water on the SCS side is relatively homogenous and appears to have the same characteristics as the Pacific water at about 2000 m (Nitani 1972; Broecker *et al.* 1986; Chen *et al.* 2001). This has been interpreted as evidence for the ventilation of the SCS by the deepwater overflow through the Luzon Strait (Qu *et al.* 2006b). Since water of Pacific origin is colder and of higher density, it sinks after crossing the Luzon Strait (Wyrtki 1961) and possibly generates a cyclonic circulation in the deep SCS (Qu *et al.* 2006b; Wang *et al.* 2011). To compensate for this descending movement, water is pulled up elsewhere by enhanced diapycnal mixing stemming from internal tides/waves, and eventually exits the SCS in the upper layer circulation. The enhanced diapycnal mixing in the SCS has been confirmed by observations, with a mean diapycnal diffusivity as large as $10^{-3}\,\mathrm{m^2\,s^{-1}}$ in magnitude (e.g. Tian *et al.* 2009). As a consequence, water entering the SCS through the deep Bashi Channel (>2000 m) can reach the upper ocean in less than 50 years, and this renewal timescale is significantly smaller than its counterpart in the Pacific (e.g. Broecker *et al.* 1986; Chen *et al.* 2001; Qu *et al.* 2006b; Li and Qu 2006).

Because of the complicated topography and the highly variable nature of the currents in the region, direct measurement of the deep-water overflow through the Luzon Strait has proven difficult. Based on a single 82-day current meter measurement, Liu and Liu (1998) showed the first observational evidence for a persistent near-bottom flow in the Luzon Strait, with a mean current speed of $0.14\,\mathrm{m\,s^{-1}}$ toward the SCS. This measurement yielded a transport estimate of 1.2 Sv in the deep layer, consistent with those derived from hydrographic data (e.g. Wang 1986; Qu *et al.* 2006b; Tian *et al.*

2006). A set of deepwater moorings was recently deployed and preliminary analysis of these data provided additional support for the existence of a deepwater overflow in the Luzon Strait (e.g., Zhou *et al.* 2014).

Water exits the SCS mainly through the Taiwan, Mindoro, and Karimata Straits. The Taiwan Strait throughflow has been extensively studied in the past several decades. Hu *et al.* (2010) provided a very comprehensive overview of prior studies. In general, three currents are involved in the Taiwan Strait throughflow: the China Coastal Current, the extension of the SCS Warm Current, and the Kuroshio branch or loop current. The net volume transport of these three currents through the Taiwan Strait exhibits a strong seasonal cycle, varying from about $2.3 + 0.82$ Sv in boreal summer to about $0.8 + 0.96$ Sv in boreal winter. Both regional monsoon and large-scale wind over the Pacific appear to play a role in generating this seasonal variability. On longer timescales, variability in the Taiwan Strait is relatively small, and nearly all of the SCSTF variability appears to occur in the Mindoro and Karimata Straits (Qu *et al.* 2006a).

In the Mindoro Strait, Wyrtki (1961) noticed that the surface flow is southward only during August–October, when the southwest monsoon prevails. It turns northward during other seasons of the year, corresponding to the northeast monsoon. The local wind becomes less important at depth. Both the North Pacific Tropical Water and Intermediate Water are clearly visible in the Sulu Sea (Frische and Quadfasel 1990; Quadfasel *et al.* 1990), suggesting an intrusion of thermocline water through the Mindoro Strait. Most of the reported transport estimates in the Mindoro Strait have been based on model outputs, falling in a range from about 0.5 to 4 Sv (e.g. Metzger and Hurlburt 1996; Lebedev and Yaremchuk 2000; Fang *et al.* 2005; Qu *et al.* 2006a; Han *et al.* 2009). Qu and Song (2009) gave an estimate of 2.4 Sv by applying the hydraulic theory to remotely sensed altimeter and ocean bottom pressure data. To our best knowledge, the only direct measurements available so far are those recently reported by Sprintall *et al.* (2012). Based on simultaneous moored time series within the Mindoro Strait (and two other small straits), they found that the mean transport through the Mindoro Strait was very small ($-0.1 + 1.1$ Sv) during 2008. They related this small transport in the Mindoro Strait to the strong La Nina event that peaked during February–March 2008. Water exiting the SCS through the Mindoro Strait can descend as deep as 570 m in the Sulu Sea (e.g. Tessler *et al.* 2010) and eventually reach the Celebes Sea through the Sibutu Passage to further affect the Pacific western boundary current and ITF (discussed in Sec. 2.3).

Water of Pacific origin also exits the SCS through the Karimata Strait (Fig. 1). Based on very limited hydrographic data, sea-level records, and ship drifts, Wyrtki (1961) first suggested an annual transport of about 0.6 Sv, with an outward flow of ~4.5 Sv in boreal winter and an inflow of ~3 Sv in boreal summer. Given the shallowness (~50 m) of the strait, it has remained controversial whether there is a significant transport through the Karimata Strait. A field experiment was recently conducted to address this problem, in which acoustic Doppler current profiler observations were carried out at two stations along a transect northwest of the Karimata Strait from December 2007 to November 2008 (Fang *et al.* 2010). One month and 10 months of full depth current data were obtained at the western and eastern stations, respectively. Analysis of these data showed that the SCS water flows persistently to the Java Sea in boreal winter. The volume transport in the month from 13 January to 12 February 2008 was estimated to be 3.6 ± 0.8 Sv. The observation confirmed the existence of the SCSTF in the Karimata Strait in boreal winter and the reversal of its transport in boreal summer. The mean transport from this observation is 0.8 Sv.

The total SCSTF transport is an issue of particular interest. In the Luzon Strait, prior studies have arrived at a broad range of transport estimates, varying from 0.5 to 10 Sv (e.g. Wyrtki 1961; Metzger and Hurlburt 1996; Lebedev and Yaremchuk 2000; Chu and Li 2000; Xue *et al.* 2004; Yaremchuk and Qu 2004; Song 2006; Yu *et al.* 2007). Recent hydrographic data favor a value near the middle of the range (Qu 2000; Qu *et al.* 2000; Tian *et al.* 2006). A common feature regarding its seasonal variability in prior studies is that the SCSTF gets stronger in boreal winter and weaker in boreal summer, which is consistent with the seasonal reversal of the monsoon. Note that the SCSTF transport can be contaminated by eddies of various timescales. Intensive eddy activities have been observed in the Luzon Strait, and they are believed to be an important process influencing the pathways of the Pacific water intrusion (e.g. Li *et al.* 1998; Hu *et al.* 2000; Wu and Chiang 2007). This has been confirmed recently by satellite-based altimeter data (e.g. Yuan *et al.* 2006; Caruso *et al.* 2006).

The SCSTF also varies on interannual-to-decadal timescales. It has been shown that the intrusion of Pacific water through the Luzon Strait depends on the strength of basin-scale winds which in turn are closely related to ENSO (e.g. Qu *et al.* 2004; Ho *et al.* 2004). An accurate estimate of the SCSTF interannual variability from observations is not available. Results from high-resolution GCMs suggest that the SCSTF intensifies during El Niño and weakens during La Nina (e.g. Qu *et al.* 2005a; Wang *et al.* 2006). On decadal timescales, the SCSTF from the model also shows a good correspondence with Pacific Decadal Oscillation (PDO), getting stronger during the positive phase of the PDO and weaker during the negative phase (e.g. Yu and Qu 2013). These results may be sensitive to the model's topography and parametrizations (e.g. Metzger and Hurlburt 2001), and require further investigation.

2.2. *The Link to the Pacific Western Boundary Current and Indonesian Throughflow*

As part of the Pacific tropical gyre (Metzger and Hurlburt 1996), the SCSTF is strongly influenced by the low-latitude western boundary current (LLWBC) in the Pacific (e.g. Qu *et al.* 2004), and the intrusion of Pacific water, in turn, may have a dramatic impact on the SCS circulation (e.g. Qu *et al.* 2005a; Wu and Chang 2005; Guan and Fang 2006; Yuan *et al.* 2007; Tozuka *et al.* 2007b, 2009). According to Sheremet's (2001) hysteresis theory, when the North Equatorial Current (NEC) bifurcation moves northward, the weakening Kuroshio east of Luzon provides a favorable condition for the intrusion of Pacific water through the Luzon Strait (Yaremchuk and Qu 2004). This probably explains why the SCSTF tends to be stronger during El Nino and the positive phase of the PDO (Qu *et al.* 2004; Yu and Qu 2013), when the NEC bifurcation moves northward (Kim *et al.* 2004; Qiu and Chen 2010). The situation during La Nina and the negative phase of the PDO is reversed.

Variability of the SCSTF may in turn affect the LLWBC in the Pacific. Results from numerical experiments have shown that transport through the Mindoro Strait can shift the NEC bifurcation by as much as 2°. With a set of numerical experiments, Metzger and Hurlburt (1996) showed that when the SCS straits are closed in their model, a greater portion of the NEC turns southward as the MC and the bifurcation point of the NEC moves northward to about 15°N. When these straits are open with no friction controlling the flow, a greater portion of the NEC turns northward as the Kuroshio east of Luzon and the bifurcation point of the NEC moves southward to about 13°N. This result implies that an enhanced SCSTF in the Mindoro Strait can result in a southward shift of the NEC bifurcation and consequently a larger

Kuroshio transport east of Luzon. The details need to be confirmed by observations.

Variability of the SCSTF may also affect the ITF. Extensive studies have been carried out on the ITF in the past decades (e.g. Wyrtki 1961; Lebedev and Yaremchuk 2000; Yaremchuk and Qu 2004; Fang *et al.* 2005 2009; Qu *et al.* 2005a; Du and Qu 2010) (also see Sec. 3). One of the most important findings in recent years is that the maximum southward velocity in the Makassar Strait, the primary pathway of the ITF, occurs at about 150 m and during the boreal winter the surface flow in the strait is very weak, leading to a considerably weaker ITF heat transport than previously thought (e.g. Vranes *et al.* 2002; Gordon *et al.* 1999, 2003, 2008). Gordon *et al.* (2003) attributed the seasonal variation of the Makassar Strait surface flow to the regional winds of the Java Sea. They argued that during the boreal winter the southeastward monsoon wind drives buoyant, low-salinity Java Sea surface water into the Southern Makassar Strait, creating a northward pressure gradient in the surface layer of the strait. This surface layer "freshwater plug" inhibits the warm surface water from the Pacific Ocean from flowing southward into the Indian Ocean. The monsoon wind reversal eliminates the obstructing pressure gradient, and as a consequence the surface flow in the Makassar Strait turns southward in the boreal summer.

Later studies (Qu *et al.* 2005a, 2006a) applied Godfrey's (1989) "island rule" to Philippine-Borne and suggested that the circulation in the Makassar Strait is a result of the interplay between the southward-flowing ITF in the thermocline and the northward-flowing SCSTF near the sea surface. Thus, it is the SCSTF instead of the local Ekman current that forces the freshwater to flow from the Java Sea to the Makassar Strait, which in turn inhibits the warm surface water from the Pacific from flowing southward. The SCSTF is mainly forced by the basin-scale wind of the Pacific (Qu *et al.* 2005a; Wang *et al.* 2006), and the local Ekman current is too weak and too shallow to account for this current. To confirm this hypothesis, Tozuka *et al.* (2007b, 2009) conducted a set of numerical experiments. Their results indicated that blocking the SCSTF in a model can enhance the southward flow near the surface and eliminate most of the vertical shear in the Makassar Strait. Results from these numerical experiments also indicated that the presence of the SCSTF can reduce the ITF heat transport in a model by as much as 47%. Although the SCSTF volume transport is only ~1 Sv in the Karimata Strait (Wyrtki 1961; Fang *et al.* 2010), about an order smaller than the ITF, its impact on the Pacific-to-Indian Ocean heat transport is expected to be larger.

Similar to what has been discussed above, Gordon *et al.* (2012) recently suggested that an increased Mindoro Strait transport during El Niño, with a commensurate increase in the southward flow of buoyant surface water through the Sulu Sea into the northern Makassar Strait, can inhibit tropical Pacific surface water injection into the Makassar Strait. Their measurements in the Makassar Strait showed dramatic changes in 2008–2009, with the characteristic thermocline velocity maximum increased from 0.7 to 0.9 $\mathrm{m\,s^{-1}}$ and shifted from 140 to 70 m, amounting to a 47% increase in the transport of warm water between 50 and 150 m during the boreal summer. They partially attributed these changes in the Makassar Strait to the La Niña event, when the SCSTF in the Mindoro Strait tends to be weaker and the effects of the freshwater plug are significantly reduced.

2.3. *Outstanding Issues*

Despite the considerable progress that has been made in the past few years, our understanding of the SCSTF is far from complete. Numerous issues and questions still remain (e.g. Qu *et al.* 2009). Most fundamental is the lack of accurate estimates of the SCSTF. As a consequence, the existing model estimates are not sufficiently constrained by observations and differ in some significant ways. How the SCSTF varies and what processes are responsible for its variability are questions that need immediate attention in future studies.

Developing coherent measurements of transports through the Luzon, Taiwan, Mindoro, and Karimata Straits is a key to this fundamental issue, and requires collaborative efforts from international communities. Given that a significant portion of the SCSTF is driven by a deep-water overflow through the Luzon strait (Qu *et al.* 2006b; Tian *et al.* 2009), vertical mixing is also an important issue to be addressed. More work needs to be done in order to get better parametrizations of diapycnal mixing for ocean models in the SCS.

Another important issue left to be addressed is the SCSTF influence on regional sea surface temperature and climate. As part of the Indonesian Maritime Continent (e.g. Ramage 1968), the SCS is recognized as a site of vigorous atmospheric convection. There, any small changes of SST can result in dramatic changes in weather patterns across the Indo-Pacific basin (e.g. Neale and Slingo 2003; McBride *et al.* 2003). With the presence of the SCSTF, variability in the SCS can further affect the sea surface temperature off Java and Sumatra, contributing directly to the coupled climate system there (Saji *et al.* 1999; Annamalai *et al.* 2003; Du *et al.* 2005). Then, how are the SCS surface temperature anomalies related to the SCSTF variability? To what extent can the SCSTF modulate the Indo-Pacific warm pool? Is the SCSTF thermodynamically active in the coupled ocean–atmosphere system of the region? If so, what is its role? In particular, can the SCSTF play a role in modulating the Southeast Asian monsoon, the Pacific ENSO, and the Indian Ocean Dipole? The existing studies summarized in this article have addressed some aspects of these questions, but most of them need to be investigated by future studies.

3. Indonesian Seas and Throughflow

The Indonesian Seas are a collection of seas that are bounded between the Indonesian Archipelago and the Australian Continent (Fig. 4). It is where the Indo-Australian Plate collides with the Eurasian Plate and thus the bottom bathymetry varies significantly; the Banda Sea is as deep as 4000 m, while the adjacent Arafura and Java Seas are as shallow as 40–80 m. The Indonesian Seas are considered to play an important role in global climate, primarily for two reasons. First, they connect the Pacific Ocean and the Indian Ocean. It is the only location near the equator where such a connection exists. A flow directed from the Pacific to the Indian Ocean is observed and is often referred to as the Indonesian Throughflow (ITF) (see Sprintall *et al.* 2004 and references therein). The ITF is a major component of inter-basin mass, heat, and freshwater exchanges (e.g. Ganachaud and Wunsch 2003) and is suggested to alter not only the oceanic condition of the equatorial Indian Ocean but also the equatorial Pacific and South Atlantic (Hirst and Godfrey 1993). Second, the Indonesian Seas are located directly underneath the region of atmospheric deep convection. Their SST plays a major role in the development of deep convections and affects the tropical atmospheric circulation (Schneider 1998). While the spatial scale of the Indonesian Seas is much smaller than those of the Pacific Ocean and the Indian Ocean, these seas are capable of influencing the tropical atmospheric circulation on the basin scale.

3.1. *Indonesian Throughflow*

The *Snellius* Expedition (1929–30) advanced the oceanographic knowledge of the Indonesian Seas significantly by providing numerous

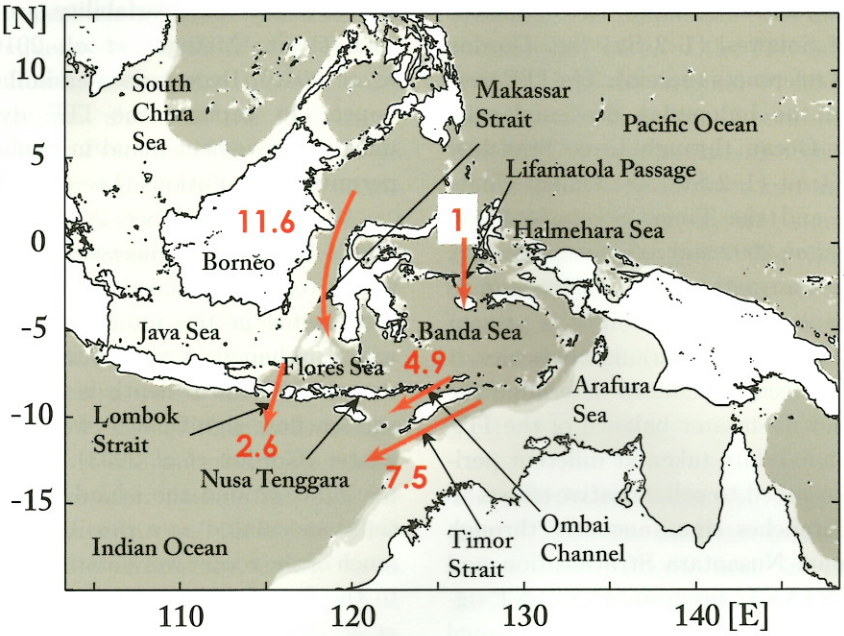

Fig. 4. Topography and coastlines of the Indonesian Seas. The red arrows are the direction of the ITF observed by INSTANT (Gordon *et al.* 2010).

hydrographic measurements and topographic data of the region (Van Aken 2005). Based on these observational data and all other data available in the region at the time, Wrytki (1961) then provided one of the most comprehensive descriptions of the surface circulation in the Indonesian Seas, which stands out even today. Moreover, the study made one of the important discoveries of the global oceanic circulation, the Indonesian Throughflow.

The ITF is a flow from the Pacific Ocean to the Indian Ocean, and a such flow that connects two global scale basins near the equator is unique to the ITF. Because the Indonesian Seas are located to the east of the Indian Ocean and potential vorticity contours in the tropical Indian Ocean are zonal, the ITF is capable of traveling across the Indian Ocean zonally (Talley and Sprintall 2005). This current, known as the Indian South Equatorial Current, will join the Agulhas current and eventually escape to the South Atlantic through the Agulhas leakage. These ITF-related currents are considered to be major components of the mass, heat, and freshwater balances for the Indian Ocean (Gordon 2005). The ITF is also suggested to make the eastern Indian Ocean warmer by advecting warm Pacific warm pool water to the Indian Ocean. Such a condition will make the Indonesian Archipelago surrounded by warm water and a region of active atmospheric convections (Schneider 1998).

The transport of the ITF is observed to be about 10–15 Sv (Gordon 2005; Sprintall *et al.* 2010) and the magnitude of the ITF is considered to be determined primarily from the wind stress curl over the South Pacific east of Australia (Godfrey 1996). The strong presence of the ITF in the oceanic climate of the Indian Ocean is partly due to the significant heat and freshwater it introduces. While the ITF is often referred to as a "flow," the actual ITF is a multibranch flow (Fig. 4). The Pacific water enters the Indonesian Seas through two branches: the Makassar Strait (8–12 Sv) and the straits east of Sulawesi (1–2 Sv) (see Gordon *et al.* 2010 and references therein). The ITF then travels around the Indonesian Seas and exits to the Indian Ocean through three branches: the Lombok Strait (1–2 Sv), the Ombai Channel (4–5 Sv), and the Timor Strait (4–8 Sv) (see Sprintall *et al.* 2009 and references therein). Note that the transport values are the annual averages. Because strong variability is present at each of the branches on various timescales, it has historically been difficult to determine the mass, heat, and freshwater balance of the ITF from observational data taken at different periods. This problem led to collaborative efforts to measure the branches simultaneously through the International Nusantara Stratification and Transport (INSTANT) program. INSTANT significantly enhanced the amount of observational data and accelerated the understanding of the ITF (e.g. Sprintall *et al.* 2009; Gordon *et al.* 2010; Pujiana *et al.* 2012).

Just as observations of the ITF have been difficult, numerical simulations of the ITF have been equally challenging. This is because simulations of the ITF require models to solve the whole of the Pacific and Indian Oceans ($\sim$10,000 km) while resolving the narrow straits of the Indonesian Archipelago ($\sim$10 km). For simulations that do not resolve the narrow straits of the Indonesian Seas, the majority of the ITF is found to pass through the Makassar Strait and the Lombok Strait (e.g. Masumoto and Yamagata 1996). This is because the boundary currents have a tendency to flow through the western most strait. Recent advances in computational power enabled basin-scale simulations with eddy-permitting and strait-resolving spatial resolutions. These models show much improvement in simulating the magnitude and variability of the ITF and appear promising in capturing the dynamics of the ITF (e.g. Masumoto *et al.* 2004; Shinoda *et al.* 2012). However, there are still some differences between the models in how well the partitioning of the ITF and the variability are captured at each strait (Metzger *et al.* 2010; Rosenfield *et al.* 2010). Recent data-assimilated products appear to capture the ITF dynamics with much improvement found in models with eddy-permitting resolutions (Lee *et al.* 2010).

As mentioned in Sec. 2.2, the vertical profile of the ITF at the Makassar Strait has been a recent topic for discussion since it is an important factor in the interbasin heat and freshwater exchange. A maximum flow speed at an around 100–150 m depth is observed, with the surface flow significantly weakening in Boreal winter (Gordon *et al.* 2003). The local freshwater input around the island of Borneo was initially speculated as a possible cause. However, much of the recent work attributes the reduction to the flow from the South China Sea. Tozuka *et al.* (2007b) suggested the importance of the flow through the Java Sea, while Gordon *et al.* (2012) suggested the flow through the Sulu Sea to be responsible. Further observations are likely necessary to validate these hypotheses but their differences may be simply due to the timescale involved. The mechanism of Gordon *et al.* (2003) and Tozuka *et al.* (2007b) is on the seasonal timescale, while that of Gordon *et al.* (2012) is on the interannual timescale.

The Indonesian Seas are the intersection of the Rossby waves from the Pacific Ocean and the Kelvin waves from the Indian Ocean (Wijffels and Myers 2000). The dynamics of these waves in the Indonesian Seas has been another topic for discussion since it will likely teach us how the ITF varies in time and how much the Pacific Ocean and the Indian Ocean are capable of communicating through the ocean. Past studies have progressed much through idealized theoretical studies but recent accumulations of observational data are enabling this topic to be examined in a more realistic scenario. Limited energy of the Rossby waves was considered to penetrate through the Indonesian Seas to the Indian Ocean (Clarke 1991) but Spall and Pedlosky (2005) showed that significant energy is likely penetrating to the Indian Ocean for shorter-frequency and smaller-scale Rossby waves. The Rossby waves are indeed found to create an annual signal in the ITF transport (Meyers 1996; Potemra 1999). The Kelvin waves, on the other hand, are found to create a semiannual signal in the ITF (Masumoto and Yamagata 1996). Observations show the Kelvin waves entering the Indonesian Seas through the Lombok Strait to the Makassar Strait (Sprintall *et al.* 2000, Pujiana *et al.* 2012), and such penetration of the Kelvin waves through narrow straits is supported by theory (Durland and Qiu 2006). However, it is still uncertain what happens to these waves after passing through the Makassar Strait. Drushka *et al.* (2010) provided a comprehensive view of how the Kelvin waves are generated in the Indian Ocean and then propagate along the southern coasts of the Nusa Tengarra on the intraseasonal timescale. They found more than half of the Kelvin wave energy to enter the Lombok Strait and the Indonesian Seas, and the remaining energy to continue along the Nusa Tengarra. Potemra and Schneider (2007) suggested the wave to dissipate by the time it reaches the Ombai Channel.

How the Indian Ocean and the Pacific Ocean interact through the ocean, especially during ENSO and the IOD, remains one of the outstanding issues that need further investigation. With improved knowledge and more available observations about the ITF and the waves entering the Indonesian Seas, we are now capable of testing various hypotheses raised in the past. It is hoped that clarifying the role of the ITF in climate would lead to improving the skills for climate variability prediction.

3.2. *Indonesian Seas*

The Indonesian Seas do not simply connect the Pacific and the Indian Ocean. Strong tidal mixing is present and thus these seas significantly modify the Pacific water before the ITF advects this water mass to the Indian Ocean. Tidal mixing in the Indonesian Seas makes the upper thermocline water of the ITF much cooler and fresher than the original Pacific water or the interior of the Indian Ocean (Gordon 2005). The SST of the region also serves as one of the major sources of heat and moisture for the development of the austral summer monsoon (Kawamura *et al.* 2002). The variability of the SST within the Indonesian Seas is considered to lead to significant changes in the magnitude of the atmospheric deep convection.

3.2.1. *Tidal Mixing*

The Indonesian Seas are where tidal waves from the Pacific and the Indian Ocean enter and dissipate (Jayne and St. Laurent 2001). As a result, the magnitude of vertical mixing there is considered much enhanced compared to other regions. Using an advection–diffusion model, Ffield and Gordon (1996) estimated that vertical mixing of the order of $10^{-4}\,\mathrm{m}^2\,\mathrm{s}^{-1}$ is likely present on the basin average. Microstructure measurements in the interior of the Banda Sea a few years later, however, showed mixing less than $10^{-5}\,\mathrm{m}^2\,\mathrm{s}^{-1}$ (Alford *et al.* 1999). This is a value similar to those found in the open ocean. Further studies eventually discovered that enhanced mixing is likely limited to where the topography is rough (e.g. Hatayama 2004; Ffield and Robertson 2005). The straits of the Halmahera Sea are also suggested to be a region of enhanced tidal mixing, which could be limiting the inflow from the South Pacific to the Indonesian Seas (Koch-Larrouy *et al.* 2007). Direct measurements are needed to evaluate these new ideas. The use of data assimilation models can also enable us to have a better spatial view of tidal mixing in the area if optimal vertical mixing coefficients can be estimated. The impact of tidal mixing can then be prescribed using such a product in various numerical models that do not resolve mixing.

Understanding the dynamics behind tidal mixing as well as determining where precisely such mixing occurs remains one of the outstanding issues. They are obviously the crucial part of understanding the role of the Indonesian Seas in global oceanic climate. Without proper tidal mixing parametrization present in the Indonesian Seas, current numerical models cannot simulate the water mass properties of the ITF even with high spatial resolution (Schiller *et al.* 1999; Masumoto *et al.* 2003).

3.2.2. *Sea Surface Temperature*

The Indonesian Seas are regions where numerical models often create warm SST bias. Because the magnitude of atmospheric convection is sensitive to the SST, this results in significant bias also for the tropical atmospheric circulation (Qu *et al.* 2005b). Understanding the oceanic dynamics in the Indonesian Seas is therefore a necessary step for improved climate simulations. The inclusion of tidal mixing, for example, is found to reduce the warm SST bias and improve the tropical atmospheric circulation (Jochum and Potemra 2008).

The warm SST of the Indonesian Seas is one of the factors behind the active atmospheric convection in the area. The seasonal cycle, however, shows the SST lower than the convective threshold during winter and warming back again in spring (Fig. 5). This cooling and warming of the SST is an important factor in the development of the Australian summer monsoon (Kawamura *et al.* 2000). The seasonal cycle of the SST is considered to be driven primarily by the monsoonal winds (Kida and Richards 2008) and the impacts from ITF and tidal mixing appear to be limited to austral summer (Kida and Wijffels 2012). The seasonally reversing monsoonal winds are also considered to play an important role in the surface heat transport back and forth in the Indian Ocean (Sprintall and Liu 2005).

The dynamics behind the annual mean and the seasonal cycle of the SST is now reasonably well understood, but the mechanism behind the interannual variability remains one of the outstanding issues (Iskandar 2010). This is partly because there are more mechanisms possible. Just as the Indonesian Seas are the intersection of basin-scale oceanic waves, they are the intersection of two large climate variabilities, ENSO and the IOD. ENSO can influence the SST and affect local precipitations (Kubota *et al.* 2010) while the SST variability can affect the development of ENSO (Annamalai *et al.* 2009). The interannual variability of the SST likely affects the onset date of the monsoon, which has large societal impacts as well (Kajikawa *et al.* 2008). Since the Indonesian Seas are where precipitation is large, freshwater input from the islands may also have an impact on the SST. The seasonal cycle of the sea surface salinity does show a strong influence of the river input from the island of Borneo (Halkides *et al.* 2010). The atmospheric condition around the Indonesian Seas has strong short-timescale variability such as the sea breeze and the MJO (e.g. Neale and Slingo 2003), and it would be interesting to learn how the ocean, atmosphere, and rivers interact on such a timescale.

4. The Kuroshio from the East China Sea Through South of Japan

As described in Sec. 2.3, most of the Kuroshio water east of Luzon Island bypasses the Luzon Strait and enters the East China Sea (ECS). The Kuroshio in the ECS starts east of Taiwan, flows along the shelf break, and ends at the Tokara Strait; the Kuroshio south of Japan starts from the Tokara Strait, flows along the southern coast of Japan, and ends southeast of Japan (Fig. 6). Sometimes, the Kuroshio south of Japan moves far away from the coast and forms a stable offshore pathway, i.e. a large meander (Kawabe 1995; LM in Fig. 6). In addition to the Kuroshio, the Ryukyu Current southeast of the Ryukyu Islands (Worthington and Kawai 1972; Nitani 1972) is also a part of the western boundary current in the northwestern Pacific.

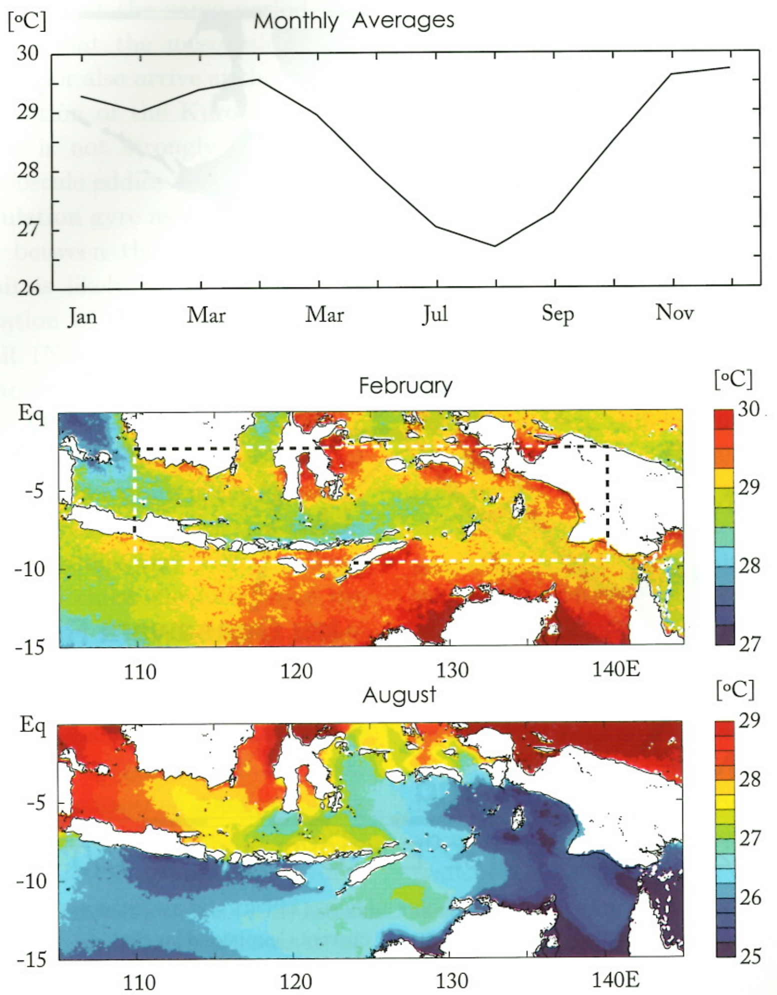

Fig. 5. Monthly averages of the SST observed in the Indonesian Seas: spatially averaged monthly SST (top), February SST (middle), and August SST (bottom). The averages are that estimated in the dotted region shown in the middle figure.

4.1. *The Kuroshio in the East China Sea*

4.1.1. *Path*

Because of strong topographic control by the shelf break, the Kuroshio has a stable path in the ECS, i.e. almost exactly following a 200 m isobath. The exception for topographic control is southwest of Kyushu, where the 200 m isobath continues northeastward and reaches 32°N but the Kuroshio changes its direction toward the Tokara Strait (Fig. 6). The dynamics of this veering of the Kuroshio path is likely associated with the baroclinity structure of the Kuroshio and its interaction with topography, namely JEBAR (joint effect of baroclinicity and bottom relief) (Guo *et al.* 2003).

Differing from the stable path along the shelf break, the Kuroshio presents an apparent seasonal variation with a range of ~50 km in its path east and northeast of Taiwan (Sun and

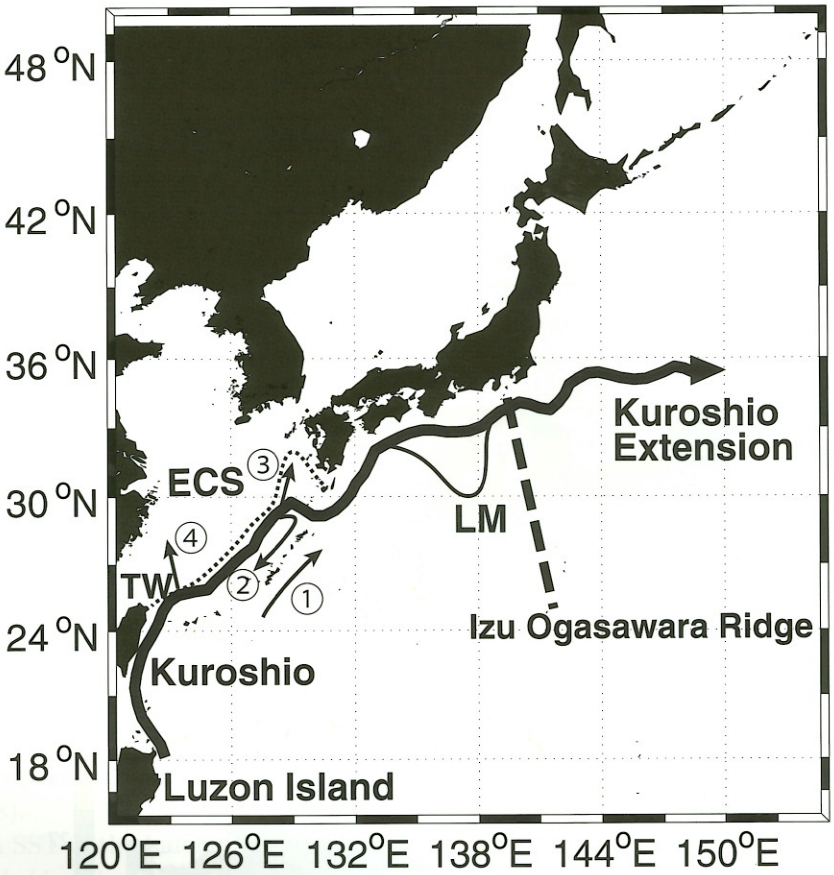

Fig. 6. Schematic diagram of the Kuroshio in the East China Sea (ECS) and south of Japan. TW denotes Taiwan; LM denotes a Large meander; numbers circled denote the currents explained in Sec. 4.1, — No. 1 is the Ryukyu Current, No. 2 is Kuroshio Counter Current, No. 3 the Kuroshio Branch Current southwest of Kyushu, and No. 4 the Kuroshio Branch Current north of Taiwan. The Broken line in the ECS indicates the 200 m isobath.

Su 1994; Tang *et al.* 2000) and southwest of Kyushu (Sun and Su 1994), which is revealed by long-term geomagnetic electrokinetograph (GEK) data (Sun and Su 1994) and a historical shipboard acoustic current profiler (Tang *et al.* 2000). The Kuroshio moves offshore (onshore) east and northeast of Taiwan and southward (northward) southwest of Kyushu in summer (winter). From the view point of the 200 m isobath, this means that the topographic control on the Kuroshio path is weak in summer but strong in winter.

In addition to seasonal variations, an offshore movement of the Kuroshio path with an order of ~50 km is found east of Taiwan and its occurrence coincides with the arrival of an anticyclonic mesoscale eddy from ocean interior (Yang *et al.* 1999). Since the anticyclonic eddy and cyclonic eddy arrive at an interval of ~100 days (Yang *et al.* 1999), it is possible that such migration occurs at the same period. An interesting thing is that the mesoscale eddies from the ocean interior also arrive at the Tokara Strait but the position of the Kuroshio inside the Tokara Strait is not strongly affected by the arrival of mesoscale eddies (Ichikawa 2001). Instead, a recirculation gyre as a cyclonic eddy inside the ECS between the shelf break and the Tokara Strait is likely responsible for the meridional migration of the Kuroshio path in the Tokara Strait (Nakamura 2005; Nakamura *et al.* 2006; Nakamura *et al.* 2012).

Although the Kuroshio presents a stable path along the shelf break between northeast of Taiwan and the separation point of the Kuroshio path from the shelf break southwest of Kyushu, the presence of front eddies and its downstream propagation may still cause meandering of the Kuroshio path. Short-term meandering variations of the Kuroshio axis in the ECS have been reported in many observational datasets, including those from short- and long-term mooring current meter records (Sugimoto *et al.* 1988; Feng *et al.* 2000; Nakamura *et al.* 2003), mooring inverted echo sounder data (James *et al.* 1999), satellite images of SST (Qiu *et al.* 1990), hydrographic data (Ichikawa and Beardsley 1993), and ocean high-frequency radar (Takahashi *et al.* 2009). These studies reported consistent characteristics of the Kuroshio axis meanders in the ECS, such as their period (10–20 days), wavelength (100–375 km), and downstream phase speed (17–30 km day^{-1}). Baroclinic instability has been proposed as a dominant process in driving the short-term Kuroshio axis meanders at the middle shelf break in the ECS (James *et al.* 1999).

4.1.2. *Transport*

The mean volume transport of the Kuroshio has a little spatial variation in the ECS. In the upstream region (east of Taiwan), its mean transport is estimated to be 21.5 Sv from the moored current meter array over a period of 1.5 year (Johns *et al.* 2001); in the downstream region (Tokara Strait), its mean transport is reported as 23.4 Sv, which is also estimated from the mooring array of the current meter and acoustic Doppler current profiler over a period of 4 years (Feng *et al.* 2000). Between the two areas, its mean transport at a section (PN line) across the Kuroshio is estimated to be 25.4 Sv from ∼40 years of hydrographic data (Hinata 1996). However, the uncertainty of these estimations is also large and the method and data period in these estimations are also different. Therefore, it is difficult to justify the above reported variations as a real change in the mean transport of the Kuroshio along its path.

The temporal variation of the Kuroshio transport shows many dominant timescales varying from intraseasonal to interannual (e.g. Minobe *et al.* 2015). According to the flat-bottomed Sverdrup theory and the change in the wind stress curl over the interior ocean, an apparent seasonal variation in the Kuroshio transport is expected (Greatbatch and Goulding 1990). However, the observations do not show an apparent seasonal variation of the Kuroshio transport east of Taiwan (Johns *et al.* 2001) and in the Tokara Strait (Feng *et al.* 2000). The only seasonal signal is reported at the PN line, where the transport varies little (less than 1.0 Sv) from winter to summer but apparently weakens (more than 3 Sv) in autumn (Hinata 1996; Shiraishi *et al.* 1999). However, this seasonal variation is different from that predicted by the Sverdrup theory. The cause for a small seasonal variation range in the Kuroshio transport in the ECS has been attributed to the intensification of Kuroshio recirculation in summer (Kagimoto and Yamagata 1997) and to the strong eddy activity in the interior ocean in May (Chang and Oey 2011), both of which increase the Kuroshio transport in the ECS in summer.

The intraseasonal variation in the Kuroshio transport has a strong relation to the arrivals of mesoscale eddies. The arrival of the westward mesoscale eddy from the interior ocean causes not only the meandering of the Kuroshio east of Taiwan but also the change in the transport of the Kuroshio east of Taiwan with a 100-day scale (Yang *et al.* 1999; Zhang *et al.* 2001). However, the conclusions on the role of anticyclonic and cyclonic eddies are not consistent in previous studies. Yang *et al.* (1999) reported that both anticyclonic and cyclonic eddies affect the Kuroshio transport east of Taiwan and an anticyclonic (cyclonic) eddy results in an increase (reduction) in the Kuroshio transport. Zhang *et al.* (2001) suggested that only the anticyclonic eddy affects the Kuroshio transport east of Taiwan and its effect is reduction in the Kuroshio transport. Kuo and Chern (2011) suggested that the interaction between the mesoscale eddy and the Kuroshio depends on the rotation direction of the eddy.

The 100-day scale variation of the current field of the Kuroshio is also found in the Tokara Strait and is associated with the mesoscale eddy east of the strait (Feng *et al.* 2000). The volume transport of the Kuroshio through the Tokara Strait has a period of approximately a half-year and is likely caused by the merger of mesoscale eddies into the Kuroshio southwest of the strait (Ichikawa 2001).

The long-term variation of the Kuroshio transport at the PN line has periods of approximately 5 years and 9 years (Saiki 1982; Shiraishi *et al.* 1999). A good correlation with zero lag has been found between the interannual variability of the Kuroshio transport and the Pacific Decadal Oscillation (PDO) (Han and Huang 2008; Andres *et al.* 2009). An interpretation of the good correlation is a barotropic response of the Kuroshio transport to the wind stress curl anomaly in the central north Pacific (Andres *et al.* 2011). Recently, a new index called the Philippines–Taiwan Oscillation (PTO) was proposed to have a close relation to the interannual variability of the Kuroshio east of Taiwan (Chang and Oey 2012).

As a warm current, the northward heat transported by the Kuroshio in the ECS is also an important issue (Bryden *et al.* 1991; Chen *et al.* 1992; Ichikawa and Chaen 2000). The heat transport calculated as a product of velocity and water temperature is 2.14 PW (Bryden *et al.* 1991), 2.76 PW (Chen *et al.* 1992), and 1.13–2.23 PW with a mean of 1.76 PW (Ichikawa and Chaen 2000). By assuming a mean temperature for southward return water and no net meridional volume transport, the meridional heat flux by the Kuroshio is to be 0.39 PW (Bryden *et al.* 1991) and 0.25–0.46 PW with a mean of 0.33 PW (Ichikawa and Chaen 2000). In addition to heat, freshwater (Ichikawa and Chaen 2000) and nutrients (Guo *et al.* 2012) are also transported by the Kuroshio in the ECS to its downstream region.

4.1.3. *Current Structure Including Countercurrents and Branch Currents*

The good agreement between the ADCP measured current shear and the geostrophic shear of the Kuroshio (Chen *et al.* 1992; Kaneko *et al.* 1993) supports the general understanding of the current structure of the Kuroshio from classical geostrophic calculation, i.e. a surface maximum speed larger than $1\,\mathrm{m\,s^{-1}}$ at its axis and gradually weakening with distance from the axis in both the horizontal and vertical directions (Nitani 1972). The seasonal variation in the geostrophic shear of the Kuroshio is not significant (Ichikawa and Beardsley 2002).

Countercurrents with an opposite direction to the Kuroshio are observed in the ECS (Fig. 6). For example, one countercurrent is reported on the inshore side of the Kuroshio northeast of Taiwan (Chuang *et al.* 1993; Tang *et al.* 1999), while another is on the offshore side of the Kuroshio southwest of Kyushu (Nitani 1972; Inoue 1981), named the Kuroshio Countercurrent (Qiu and Imasato 1990; No. 2 in Fig. 6). The countercurrent exists also near the bottom of shelf break (Chen *et al.* 1992; Nakamura *et al.* 2008) and its presence is proposed to be related to eddy activities (Chen *et al.* 1992; Ichikawa and Beardsley 2002).

On the other hand, branch currents with approximately the same direction as the Kuroshio are also one important feature of the current system in the ECS. The Kuroshio Branch Current north of Taiwan (No. 4 in Fig. 6) is recognized in a surface current map based on historical GEK data (Qiu and Imasato 1990), observed by long-term moored current meter data (Tang and Yang 1993; Liang *et al.* 2003), and examined by a two-layer theoretical model (Hsueh *et al.* 1993) and three-dimensional numerical models (Guo *et al.* 2006; Yang *et al.* 2011; 2012). Another branch current, the Kuroshio Branch Current west of Kyushu (No. 3 in Fig. 6), was also recognized many decades ago (Nitani 1972), observed by surface drifters (Lie *et al.* 1998), and examined by two-layer models (Hsueh *et al.* 1996; Isobe 2000) and a numerical model (Guo *et al.* 2006).

Although not inside the ECS, the Ryukyu Current (No. 1 in Fig. 6) can also be considered a branch current along with the Kuroshio in the ECS (Andres *et al.* 2008). The presence of the Ryukyu Current has been realized many decades ago (Worthington and Kawai 1972; Nitani 1972) and was confirmed in the current field from ADCP and hydrographic data (Yuan *et al.* 1998) and from moored data by the Inverted Echo Sounder with pressure gauge (PIES). The volume transport of the Ryukyu Current has been estimated by combination of PIES or ADCP data with a satellite altimeter (Zhu *et al.* 2003, 2004; Ichikawa *et al.* 2004; Andres *et al.* 2008). Its mean transport is 4.5 Sv at a section southeast of Okinawa Island (Zhu *et al.* 2004) but 17.5 Sv at a section southeast of Amami-Ohshima Island, showing a large spatial variation in the Ryukyu Current. The standard deviations of 5.5 Sv (Zhu *et al.* 2004) and 11.4 Sv (Ichikawa *et al.* 2004) at two sections suggest a large temporal variation in the Ryukyu Current. Activities of the mesoscale eddy and the strength of recirculation have been considered as causes of such larger spatial and temporal variations in the Ryukyu Current (Zhu *et al.* 2004; Ichikawa *et al.* 2004; Andres *et al.* 2008).

The Kuroshio in the ECS and the Ryukyu Current meet south of Kyushu and their combination contributes to the Kuroshio south of Japan (Andres *et al.* 2008), which is the topic of the next subsection. On the other hand, the Kuroshio in the ECS significantly affects the circulations and nutrient dynamics over the shallow continental shelf of the ECS (Matsuno *et al.* 2009; Zhao and Guo 2011). For those topics, three comprehensive reviews (Ichikawa and Beardsley 2002; Isobe 2008; Chen 2008) are available.

4.2. *The Kuroshio South of Japan*

The bimodality of stable Kuroshio paths south of Japan is unique among various types of the western boundary current variability. The two typical stable paths — the large meander and nonlarge meander paths — persist from a few years to a decade (Kawabe 1995). The bimodality has been investigated by many scientists from both the theoretical and observational viewpoints, especially after raising a theoretical interest by Robison and Taft (1972). Theoretical studies (e.g. Masuda 1982) suggested that the Kuroshio may possess multiple equilibria under an external condition. Kawabe (1995) showed on the basis of tide gauge observation that either the large meander or nonlarge meander state appeared when the upstream volume transport was larger than or the same as its climatological mean. Kurogi and Akitomo (2003) suggested that the multiple equilibrium states of the Kuroshio path may have been established by the wind stress field in the North Pacific over the past 40 years. Kurogi and Akitomo (2006) and Akitomo (2008) proposed an interesting working hypothesis on the possible range of the averaged wind stress amplitude allowing the multiple equilibrium and its interdecadal modulation by change of the basic stratification.

Dynamic balance between the advection and beta terms in the potential vorticity conservation equation associated with stationary Rossby waves is proposed as a fundamental maintenance mechanism of the Kuroshio large meander state (White and McCreary 1976). The roles of physical parameters, including the Izu–Ogasawara Ridge, the continental slope along the south of Japan, the inclination of coastal topography, inflow velocity and transport, and stratification in the stability of the Kuroshio paths, have been examined by many studies (e.g. Chao 1984; Yasuda *et al.* 1985; Yoon and Yasuda 1987; Yamagata and Umatani 1989; Sekine 1990; Akitomo *et al.* 1991, 1997; Mitsudera and Grimshaw 1994; Masuda *et al.* 1999, 2000; Mitsudera *et al.* 2006).

The existence of disturbances triggering the transitions between the stable paths was suggested from the *in-situ* data analysis (Kawabe 1995). Mesoscale eddy activity was recognized as one of the possible origins of the trigger phenomena by studies using the satellite data analysis (Ebuchi and Hanawa 2003) and model simulations (Endoh and Hibiya 2001; Miyazawa *et al.* 2004; 2005; Tsujino *et al.* 2006). Recently, the Kuroshio took the large meander path from summer 2004 to summer 2005 after the nonlarge meander period of 13 years. These bidirectional transitions between nonlarge meander and large meander were the first events that were fully monitored by the satellite altimeters. Several data assimilation studies combining the state-of-the-art ocean general circulation models and altimeter data examined the formation (Usui *et al.* 2008a,b; Miyazawa *et al.* 2008) and decay (Usui *et al.* 2011) processes, strongly suggesting the actual roles of mesoscale eddies originating from the upstream region around the subtropical front in the real Kuroshio path transitions.

Detailed analyses of the large meander event in 2004 shed light on the roles of the local processes in particular the Koshu Seamount south of Japan (Tsujino *et al.* 2006; Endoh *et al.* 2009; 2011) in the formation of the large meander associated with a deep anticyclonic eddy enhanced by the bottom slope. The basin-scale process that could be responsible for the mesoscale eddy activity triggering the Kuroshio path transitions was proposed by Chang and Oey (2012), who suggested the interannual variation of the dipole structure of the wind stress curl around the Philippines and Taiwan. Interestingly, a long-term global eddy-resolving model simulation (Elizabeth *et al.* 2012) reproduced the realistic Kuroshio path transitions between large meander and nonlarge meander even if the external forcings of the wind stress and heat flux did not include any kind of interannual variations, suggesting the importance of intrinsic variability of the deep anticyclone around the Koshu Seamount.

4.3. *Outstanding Issues*

As described above, there have been many studies of the Kuroshio from the ECS through the area south of Japan. However, most studies focused on only one area of the Kuroshio. Consequently, our understanding of the downstream variations of the Kuroshio transport along its long pathway is not sufficient. In addition, the joining of the Ryukyu Current and the Kuroshio recirculation (Imawaki *et al.* 2001) into the Kuroshio main stream makes this issue more complex. In the future, more studies will be necessary to examine the geographical connection of the Kuroshio transport from its upstream area to its downstream area and the connection of the Kuroshio transport to the Ryukyu Current and Kuroshio recirculation, not only for a steady state but also for a variety of timescales.

Among several important timescales for the temporal variations of the Kuroshio, the understanding of the interannual variations of the Kuroshio transport and their associated variations in water mass propoties such as water temperature, salinity, nutrients, and dissolved oxygen is far from a sufficient level. With accumulation of satellite and Argo data and improvement of the computer environment, which make long-term runs of numerical model easier, many comprehensive researches on this issue can be expected.

The Kuroshio transports a huge amount of heat from the tropical to the subtropical–subarctic Pacific Ocean, and thus could activate intensive basin-scale air–sea interactions. Recent studies (Nonaka and Xie 2003; Sugimoto and Hanawa 2012; Nakamura *et al.* 2012) strongly suggest the active roles of the Kuroshio and its path transitions south of Japan in the air–sea interactions near Japan. Further intensive studies toward this research direction are also needed in the near future.

References

Adler, R. F., G. J. Huffman, A. Chang, R. Ferraro, P. Xie, J. Janowiak, B. Rudolf, U. Schneider, S. Curtis, D. Bolvin, A. Gruber, J. Susskind, P. Arkin, and E. Nelkin, 2003: The Version 2 Global Precipitation Climatology Project (GPCP) Monthly Precipitation Analysis (1979-present), *J. Hydrometeor*, **4**, 1147–1167.

Akitomo, K., T. Awaji, and N. Imasato, 1991: Kuroshio path variation south of Japan. 1 Barotropic inflow–outflow model. *J. Geophys. Res.*, **96**, 2549–2560.

Akitomo, K., S. Masuda, and T. Awaji, 1997: Kuroshio path variation south of Japan: stability of the paths in a multiple equilibrium regime. *J. Oceanogr.*, **53**, 129–142.

Akitomo, K., 2008: Effects of stratification and mesoscale eddies on Kuroshio path variation south of Japan. *Deep Sea Res. I*, **55**, 997–1008.

Alford, M. H., M. C. Gregg, and M. Ilyas, 1999: Diapycnal mixing in the Banda Sea: results of the first microstructure measurements in the Indonesian Throughflow. *Geophys. Res. Lett.*, **26**(17), 2741–2744, doi:10.1029/1999GL002337.

Andres, M., J.-H. Park, M. Wimbush, X.-H. Zhu, K.-I. Chang, and H. Ichikawa, 2008: Study of the Kuroshio/Ryukyu Current system based on satellite–altimeter and *in situ* data measurements. *J. Oceanogr.*, **64**, 937–950.

Andres, M., J.-H. Park, M. Wimbush, X. Zhu, H. Nakamura, K. Kim, and K.-I. Chang, 2009: Manifestation of the Pacific Decadal Oscillation in the Kuroshio. *Geophys. Res. Lett.*, **36**, L16602, doi:10.1029/2009GL039216.

Andres, M., Y.-O. Kwon, and J. Yang, 2011: Observations of the Kuroshio's barotropic and baroclinic response to basin-wide wind forcing. *J. Geophys. Res.*, **116**, C04011, doi:10.1029/2010JC006863.

Annamalai, H., R. Murtugudde, J. Potemra, S. P. Xie, P. Liu, and B. Wang, 2003. Coupled dynamics over the Indian Ocean: spring initiation of the Zonal Mode. *Deep Sea Res. II*, **50**, 2305–2330.

Annamalai, H., S. Kida, and J. Hafner, 2010: Potential Impact of the tropical Indian Ocean–Indonesian Seas on El Nino characteristics. *J. Clim.*, **23**, 3933–3952.

Battisti, D. S. and A. C. Hirst, 1989: Interannual variability in a tropical atmosphere–ocean model: influence of the basic state, ocean geometry and nonlinearity. *J. Atmos. Sci.*, **46**, 1687–1712.

Behringer, D. W. and Y. Xue, 2004: Evaluation of the global ocean data assimilation system at NCEP: the Pacific Ocean. *Eighth Symposium on Integrated Observing and Assimilation Systems for Atmosphere, Oceans, and Land Surface*, AMS 84th Annual Meeting, Washington State Convention and Trade Center, Seattle, Washington, 11–15.

Boulanger, J.-P., S. Cravatte, and C. Menkes, 2003: Reflected and locally wind-forced interannual equatorial Kelvin waves in the western Pacific Ocean. *J. Geophys. Res.*, **108**, 3311, doi:10.1029/2002JC001760.

Broecker, W. S., W. C. Patzert, J. R. Toggweiler, and M. Stuive, 1986. Hydrography, chemistry, and radioisotopes in the southeast Asian basins. *J. Geophys. Res.*, **91**, 14,345–14,354.

Broecker, W. S., 1991: The great ocean conveyor. *Oceanogr.*, **4**, 79–89.

Bryden, H. L., D. H. Roemmich, and J. A. Church, 1991: Ocean heat transport across 24°N in the Pacific. *Deep Sea Res.*, **38**, 297–324.

Caruso, M. J., G. G. Gawarkiewicz, and R. Beardsley, 2006. Interannual variability of the Kuroshio intrusion in the South China Sea. *J. Oceanogr.* **62**, 559–575.

Chang, P., T. Yamagata, P. Schopf, S. K. Behera, J. Carton, W. S. Kessler, G. Meyers, T. Qu, F. Schott, S. Shetye, and S.-P. Xie, 2006: Climate fluctuations of tropical coupled systems — the role of ocean dynamics. *J. Clim.*, **19**, 5122–5174.

Chang, Y. L. and L. Y. Oey, 2011: Interannual and seasonal variations of Kuroshio transport east of Taiwan inferred from 29 years of tide-gauge data. *Geophys. Res. Lett.*, **38**, L08603.

Chang, Y.-L. and L.-Y. Oey, 2012: The Philippines–Taiwan oscillation: monsoonlike interannual oscillation of the subtropical–tropical western north Pacific wind system and its impact on the ocean. *J. Clim.*, **25**, 1597–1618.

Chao, S.-Y., 1984: Bimodality of the Kuroshio. *J. Phys. Oceanogr.*, **14**, 92–103.

Chao, S.-Y., P. T. Shaw, and S. Y. Wu, 1996: Deep water ventilation in the South China Sea. *Deep Sea Res. I*, **43**(4), 445–466.

Chen, C., R. C. Beardsley, and R. Limeburner, 1992: The structure of the Kuroshio southwest of Kyushu: velocity, transport, and potential vorticity fields. *Deep Sea Res.*, **39**, 245–268.

Chen, C.-T. and M. H. Huang, 1996: A mid-depth front separating the South China Sea water and the Philippine Sea water. *J. Oceanogr.*, **52**, 17–25.

Chen, C.-T., S. L. Wang, B. J. Wang, and S. C. Pai, 2001: Nutrients budgets for the South China Sea basin. *Mari. Chem.*, **75**, 281–300.

Chen, C. T., 2008: Distributions of nutrients in the East China Sea and the South China Sea connection. *J. Oceanogr.*, **64**, 737–751.

Chen, Z. and L. Wu, 2011: Dynamics of the seasonal variation of the North Equatorial Current bifurcation. *J. Geophys. Res.*, **116**, C02018, doi:10.1029/2010JC006664.

Chen, Z. and L. Wu, 2012: Long-term change of the Pacific North Equatorial Current bifurcation in SODA. *J. Geophys. Res.*, **117**, C06016, doi:10.1029/2011JC007814.

Chow, C. H. and Liu, Q., 2012: Eddy advective effects on the temperature and wind speed of the sea surface in the Northwest Pacific Subtropical Countercurrent area from satellite observations. *Int. J. Remote Sens.*, **34**(2), 600–612, doi:10.1080/01431161.2012.715775.

Chu, P. and R. Li, 2000. South China Sea isopycnal-surface circulation. *J. Phys. Oceanogr.*, **30**, 2419–1438.

Chuang, W. S., H. W. Li, T. Y. Tang, and C. K. Wu, 1993: Observations of the countercurrent on the inshore side of the Kuroshio northeast of Taiwan. *J. Oceanogr.*, **49**, 581–592.

Clarke, A. J., 1991: On the reflection and transmission of low-frequency energy at the irregular western Pacific ocean boundary. *J. Geophy. Res.*, **96**, 3289–3305.

Cronin, M. F. and M. J. McPhaden, 2002: Barrier layer formation during westerly wind bursts. *J. Geophys. Res.*, **107**, 8020, doi:10.1029/2001JC001171.

Delcroix, T. and M. J. McPhaden, 2002: Interannual sea surface salinity and temperature changes in the western Pacific warm pool during 1992–2000. *J. Geophys. Res.*, **107**, 8002, doi:10.1029/2001JC000862.

Du, Y., T. Qu, G. Meyers, Y. Masumoto, and H. Sasaki, 2005: Seasonal heat budget in the mixed layer of the southeastern tropical Indian Ocean in a high-resolution global general circulation model. *J. Geophys. Res.*, **110**, C04012, doi:10.1029/2004JC002845.

Du, Y. and T. Qu, 2010: Three inflow pathways of the Indonesian throughflow as seen from the simple ocean data assimilation. *Dyna. Atmos. Oceans*, **50**, 233–256.

Drushka, K., J. Sprintall, S. T. Gille, and I. Brodjonegoro, 2010: Vertical structure of Kelvin waves in the Indonesian Throughflow exit passages. *J. Phys. Oceanogr.*, **40**, 1965–1987, doi:10.1175/2010JPO4380.1.

Durland, T. S., B. Qiu, 2003: Transmission of subinertial Kelvin waves through a strait. *J. Phys. Oceanogr.*, **33**, 1337–1350, doi:10.1175/1520-0485(2003)033<1337:TOSKWT>2.0.CO;2.

Ebuchi, N. and K. Hanawa, 2003: Influence of mesoscale eddies on variations of the Kuroshio path south of Japan. *J. Oceanogr.*, **59**, 25–36.

Eisenman, I., L. Yu, and E. Tziperman, 2005: Westerly wind bursts: ENSO's tail rather than the dog? *J. Clim.*, **18**, 5224–5238.

Elizabeth, M. D., S. R. Jayne, F. O. Bryan, S. Peacock, and M. Maltrud, 2012: Kuroshio pathways in a climatologically forced model. *J. Oceanogr.*, **68**, 625–639.

Endoh, T. and T. Hibiya, 2001: Numerical simulation of the transient response of the Kuroshio leading to the large meander formation south of Japan. *J. Geophys. Res.*, **106**, 26,833–26,850.

——— and ———, 2009: Interaction between the trigger meander of the Kuroshio and the abyssal anticyclone over Koshu Seamount as seen in the reanalysis data. *Geophys. Res. Lett.*, **36**, L18604, doi:10.1029/2009GL039389.

Endoh, T., H. Tsujino, and T. Hibiya, 2011: The effect of Koshu Seamount on the formation of the Kuroshio large meander south of Japan. *J. Phys. Oceanogr.*, **41**, 1624–1629. .

Fang, G., D. Susanto, I. Soesilo, Q. Zheng, F. Qiao, and Z. Wei, 2005: A note on the South China Sea shallow interocean circulation. *Adv. Atmos. Sci.*, **22**, 945–954.

Fang, G., Y. Wang, Z. Wei, Y. Fang, F. Qiao, and X. Hu, 2009: Interocean circulation and heat and freshwater budgets of the South China Sea based on a numerical model. *Dynam. Atmos. Oceans*, **47**(1–3), 55–72, doi:10.1016/j.dynatmoce.2008.09.003.

Fang, G., R. D. Susanto, S. Wirasantosa, F. Qiao, A. Supangat, B. Fan, Z. Wei, B. Sulistiyo, and S. Li, 2010: Volume, heat, and freshwater transports from the South China Sea to Indonesian seas in the boreal winter of 2007–2008. *J. Geophys. Res.*, **115**, C12020, doi:10.1029/2010JC006225.

Feng, M., H. Mitsudera, and Y. Yoshikawa, 2000: Structure and variability of Kuroshio current at the Tokara Strait. *J. Phys. Oceanogr.*, **30**, 2257–2276.

Ffield, A. and A. L. Gordon, 1996: Tidal mixing signatures in the Indonesian Seas. *J. Phys. Oceanogr.*, **26**(C10), 1924–1937.

Ffield, A. and R. Robertson, 2005: Indonesian Seas fine structure variability. *Oceanography*, **18**, 108–111.

Firing, E., Y. Kashino, and P. Hacker, 2005: Energetic subthermocline currents observed east of Mindanao. *Deep Sea Res. II*, **52**, 605–613.

Frische, A. and D. Quadfasel, 1990: Hydrography of the Sulu Sea. *Proceedings of the Ocean Drilling Program, Initial Reports*, **124**, 101–104. College Station, TX; eds. C. Rangin, E. Silver, M. T. von Breymann, *et al.*

Gan, J., H. Li, E. N. Curchitser, and D. B. Haidvogel, 2006: Modeling South China Sea circulation: response to seasonal forcing regimes, *J. Geophys. Res.*, **111**, C06034, doi:10.1029/2005JC003298.

Ganachaud, A. and C. Wunsch, 2003: Large-scale ocean heat and freshwater transports during the World Ocean Circulation Experiment. *J. Clim.*, **16**, 696–705.

Gao, S., T. Qu, and D. Hu, 2012: Origin and pathway of the Luzon Undercurrent identified by a simulated adjoint tracer. *J. Geophys. Res.*, **117**, G05011, doi:10.1029/2011JC007748.

Godfrey, J. S., 1989: A Sverdrup model of the depth-integrated flow for the world ocean allowing for island circulations. *Geophys. Astrophys. Fluid Dynam.*, **45**, 89–112.

Godfrey, J. S., 1996: The effect of the Indonesian throughflow on ocean circulation and heat exchange with the atmosphere: A review. *J. Geophys. Res.*, **101**, 12,217–12,237.

Gordon, A. L. and V. M. Kamenkovich, 2010: "Modelling and observing the Indonesian Throughflow," a special issue of dynamics of atmosphere and ocean. *Dynam. Atmos. Oceans*, **50**, 113–114.

Gordon, A. L., 1986: Interocean exchange of thermocline water. *J. Geophys. Res.*, **91**, 5037–5046.

Gordon, A. L., R. D. Susanto, and A. L. Ffield, 1999: Throughflow within Makassar Strait. *Geophys. Res. Lett.*, **26**, 3325–3328, doi:10.1029/1999GL002340.

Gordon, A. L., R. D. Susanto, and K. Vranes, 2003: Cool Indonesian throughflow as a consequence of restricted surface layer flow. *Nature*, **425**, 824–828.

Gordon, A. L., 2005: Oceanography of the Indonesian Seas and their throughflow. *Oceanography*, **18**, 14–27.

Gordon, A. L., R. D. Susanto, A. Ffield, B. A. Huber, W. Pranowo, and S. Wirasantosa, 2008: Makassar Strait throughflow, 2004 to 2006. *Geophys. Res. Lett.*, **35**, L24605, doi:10.1029/2008GL036372.

Gordon, A. L., J. Sprintall, H. M. Van Aken, D. Susanto, S. Wijffels, R. Molcard, A. Ffield, W. Pranowo, and S. Wirasantosa, 2010: The Indonesian Throughflow during 2004–2006 as observed by the INSTANT program. *Dynam. Atmos. Oceans*, **50**, 115–128.

Gordon, A. L., B. A. Huber, E. J. Metzger, R. D. Susanto, H. E. Hurlburt, and T. R. Adi, 2012: South China Sea throughflow impact on the Indonesian throughflow. *Geophys. Res. Lett.*, **39**, L11602, doi:10.1029/2012GL052021.

Graham, N. E. and T. P. Barnettk, 1987: Sea surface temperature, surface wind divergence, and convection over tropical oceans. *Science*, **238**, 657–659.

Greatbatch, R. J. and A. Goulding, 1990: On the seasonal variation of transport through the Tokara Strait. *J. Oceanogr. Soc. Jpn.*, **46**, 9–20.

Guan, B. and G. Fang, 2006: Winter counter-wind currents off the Southeastern China coast: a review. *J. Oceanogr.*, **62**, 1–24.

Guo, Z., 1985: Wintertime South China Sea Warm Current and the westward current on its right. *Trop. Oceanolo.*, **4**, 1–9 (in Chinese, with English abstract).

Guo, X. Y., H. Hukuda, Y. Miyazawa, and T. Yamagata, 2003: A triply nested ocean model for simulating the Kuroshio: roles of horizontal resolution on JEBAR. *J. Phys. Oceanogr.*, **33**(1), 146–169.

Guo, X. Y., Y. Miyazawa, and T. Yamagata, 2006: The Kuroshio onshore intrusion along the shelf break of the East China Sea: the origin of the Tsushima Warm Current. *J. Phys. Oceanogr.*, **36**(12), 2205–2231.

Guo, X. Y., X. H. Zhu, Q. S. Wu, and D. Huang, 2012: The Kuroshio nutrient stream and its temporal variation in the East China Sea. *J. Geophys. Res.-Oceans*, **117**, C01026, doi:10.1029/2011JC007292.

Halkides, D., T. Lee, and S. Kida, 2011: Mechanism controlling the seasonal mixed-layer temperature and salinity of the Indonesian Seas. *Ocean Dynam.*, **61**, 481–495, doi:10.1007/s10236-010-0374-3.

Han, G. and W. Huang, 2008: Pacific decadal oscillation and sea level variability in the Bohai, Yellow, and East China seas. *J. Phys. Oceanogr.*, **38**, 2772–2783, doi:10.1175/2008JPO3885.1.

Han, W., A. M. Moore, J. Levin, B. Zhang, H. G. Arango, E. Curchitser, E. D. Lorenzo, A. L. Gordon, and J. Lin, 2009: Seasonal surface ocean circulation and dynamics in the Philippine archipelago region during 2004–2008. *Dynam. Atmos. Oceans*, **47**, 114–137.

Harrison, D. E. and G. A. Vecchi, 1997: Westerly wind events in the tropical Pacific, 1986–95. *J. Clim.*, **10**, 3131–3156.

Halkides, D., T. Lee, and S. Kida, 2011: Mechanism controlling the seasonal mixed-layer temperature and salinity of the Indonesian Seas. *Ocean Dynam.*, **61**, 481–495, doi:10.1007/s10236-010-0374-3.

Hasegawa, T., K. Ando, K. Mizuno, and R. Lukas, 2009: Coastal upwelling along the north coast of Papua New Guinea and SST cooling over the Pacific warm pool: a case study for the 2002/03 El Niño event. *J. Oceanogr.*, **65**, 817–833.

Hasegawa, T., K. Ando, K. Mizuno, R. Lukas, B. Taguchi, and H. Sasaki, 2010: Coastal upwelling along the north coast of Papua New Guinea and El Niño events during 1981–2005. *Ocean Dynam.*, **60**, 1255–1269.

Hatayama, T., 2004: Transformation of the Indonesian Throughflow water by vertical mixing and its relation to tidally generated internal waves. *J. Oceanogr.*, **60**, 569–585, doi:10.1023/B:JOCE.0000038350.32155.cb.

Hinata, T., 1996: Seasonal variation and long-term trends of the oceanographic conditions along a fixed hydrographic line crossing the Kuroshio in the East China Sea. *Oceanogr. Mag.*, **45**, 9–32.

Ho, C.-R., Q. Zheng, N.-J. Kuo, C.-H. Tsai, and N. E. Huang, 2004: Observation of the Kuroshio intrusion region in the South China Sea from AVHRR data. *Int. J. Remote Sens.* **25**, 4583–4591.

Hirst, A. C. and J. S. Godfrey, 1993: The role of Indonesian Throughflow in a global ocean GCM. *J. Phys. Oceanogr.*, **23**, 1057–1086.

Hsueh, Y., C.-S. Chern, and J. Wang, 1993: The blocking of the Kuroshio by the continental shelf northeast of Taiwan. *J. Geophys. Res.*, **98**, 12351–12359.

Hsueh, Y., H.-J. Lie, and H. Ichikawa, 1996: On the branching of the Kuroshio west of Kyushu. *J. Geophys. Res.*, **101**(C2), 3851–3857.

Hsueh, Y., and L. Zhong, 2004: A pressure-driven South China Sea warm current. *J. Geophys. Res.*, **109**, C09014, doi:10.1029/2004JC002374.

Hu, D., and M. Cui, 1989: The western boundary current of the Pacific and its role in climate. *Chin. J. Oceanol. Limnol.*, **9**, 1–14.

Hu, J., H. Kawamura, H. Hong, and Y. Qi, 2000. A review on the currents in the South China Sea: seasonal circulation, South China Sea warm current, and Kuroshio intrusion. *J. Oceanogr.*, **56**, 607–624.

Hu, J., H. Kawamura, C. Li, H. Hong, and Y. Jiang, 2010: Review on current and seawater volume transport through the Taiwan Strait. *J. Oceanogr.*, **66**, 591–610.

Ichikawa, K., 2001: Variation of the Kuroshio in the Tokara Strait induced by meso-scale eddies. *J. Oceanogr.*, **57**, 55–68.

Ichikawa, H. and R. C. Beardsley, 1993: Temporal and spatial variability of volume transport of the Kuroshio in the East China Sea. *Deep Sea Res.*, **40**, 583–605.

Ichikawa, H. and M. Chaen, 2000: Seasonal variation of heat and freshwater transports by the Kuroshio in the East China Sea. *J. Mar. Sys.*, **24**, 119–129.

Ichikawa, H. and R. Beardsley, 2002: The current system in the Yellow and East China Seas. *J. Oceanogr.*, **58**, 77–92.

Ichikawa, H., H. Nakamura, A. Nishina, and M. Higashi, 2004: Variability of north-eastward current southeast of northern Ryukyu Islands. *J. Oceanogr.*, **60**, 351–363.

Imawaki, S., U. Hiroshi, H. Ichikawa, M. Fukazawa, S. Umatani, and ASUKA Group, 2001: Satellite altimeter monitoring the Kuroshio transport south of Japan. *Geophys. Res. Lett.*, **28**, 17–20.

Ishida, A., Y. Kashino, S. Hosoda, and K. Ando, 2008: North–south asymmetry of warm water volume transport related with El Niño variability. *Geophys. Res. Lett.*, **35**, L18612, doi:10.1029/2008GL034858.

Iskandar, I., 2010: Seasonal and interannual patters of sea surface temperature in Banda Sea as revealed by self-organizing map. **30**, 1136–1148.

Isobe, A., 2000: Two-layer model on the branching of the Kuroshio southwest of Kyushu. *Jpn. J. Phys. Oceanogr.*, **30**, 2461–2476.

Isobe, A., 2008: Recent advances in ocean-circulation research on the Yellow Sea and East China Sea shelves. *J. Oceanogr.*, 64, 569–584.

James, C., M. Wimbush, and H. Ichikawa, 1999: Kuroshio meanders in the East China Sea. *J. Phys. Oceanogr.*, **29**, 259–272.

Jayne, S. R. and L. C. St. Laurent, 2001: Parameterizing tidal dissipation over rough topography. *Geophys. Res. Lett.*, **28**, 811–814.

Johns, W. E., T. N. Lee, D. X. Zhang, R. Zantopp, C. T. Liu, and Y. Yang, 2001: The Kuroshio east of Taiwan: moored transport observations from the WOCE PCM-1 array. *J. Phys. Oceanogr.*, **31**(4), 1031–1053.

Jochum, M. and J. Potemra, 2008: Sensitivity of tropical rainfall to Banda Sea diffusivity in the Community Climate System Model. *J. Clim.*, **21**, 6445–6454.

Johns, W. E., T. N. Lee, D. X. Zhang, R. Zantopp, C. T. Liu, and Y. Yang, 2001: The Kuroshio east of Taiwan: moored transport observations from the WOCE PCM-1 array. *J. Phys. Oceanogr.*, **31**(4), 1031–1053.

Kagimoto, T. and T. Yamagata, 1997: Seasonal transport variations of the Kuroshio: an OGCM simulation. *J. Phys. Oceanogr.*, **27**, 403–418.

Kaneko, A., N. Gohda, W. Koterayama, M. Nakamura, S. Mizuno, and H. Furukawa, 1993: Towed ADCP fish with depth and roll controllable wings and its application to the Kuroshio observation. *J. Oceanogr.*, **49**, 383–395.

Kashino, Y., A. Ishida, and Y. Kuroda, 2005: Variability of the Mindanao Current: mooring observation results. *Geophys. Res. Lett.*, **32**, L18611, doi:10.1029/2005GL023880.

Kashino, Y., I. Ueki, Y. Kuroda, and A. Purwandani, 2007: Ocean variability north of New Guinea derived from TRITON buoy data. *J. Oceanogr.*, **63**, 545–559.

Kashino, Y., N. España, F. Syamsudin, K. J. Richards, T. Jensen, P. Dutrieux, and A. Ishida, 2009: Observations of the North Equatorial Current, Mindanao Current, and Kuroshio Current system during the 2006/07 El Niño and 2007/08 La Niña. *J. Oceanogr.*, **65**, 325–333.

Kashino, Y., A. Ishida, and S. Hosoda, 2011: Observed ocean variability in the Mindanao Dome region. *J. Phys. Oceanogr.*, **41**, 287–302.

Kawamura, R., Y. Fukuta, H. Ueda, T. Matsuura, and S. Iizuka, 2002: A mechanism of the onset of the Australia summer monsoon. *J. Geophys. Res.*, **107**(D14), 4204, doi:10.1029/2001JD001070.

Kawabe, M., 1995: Variations of current path, velocity, and volume transport of the Kuroshio in relation with the large meander. *J. Phys. Oceanogr.*, **25**, 3103–3117.

Kida, S. and K. J. Richards, 2009: Seasonal sea surface temperature variability in the Indonesian Seas. *J. Geophys. Res.*, **114**, C06016, doi:10.1029/2008JC005150.

Kida, S. and S. Wijffels, 2012: The impact of the Indonesian Throughflow and tidal mixing on the summertime sea surface temperature in the western Indonesian Seas. *J. Geophys. Res.*, **117**, C09007, doi:10.1029/2012JC008162.

Kim, H., S. Kimura, A. Shinoda, T. Kitagawa, Y. Sasai, and H. Sasaki, 2007: Effect of El Niño on migration and larval transport of the Japanese eel (*Anguilla japonica*). *ICES J Mar. Sci.*, **64**, 1387–1395.

Kim, Y. Y., T. Qu, T. Jensen, T. Miyama, H. W. Kang, H. Mitsudera, and A. Ishida, 2004: Seasonal and interannual variations of the NEC bifurcation in a high-resolution OGCM. *J. Geophys. Res.*, **109**, 3040, doi:10.1029/2003JC002013.

Kobashi, F., H. Mitsudera and S.-P. Xie, 2006: Three subtropical fronts in the North Pacific: observational evidence for mode water-induced subsurface frontogensis. *J. Geophys. Res. Oceans*, **111**, C09033, doi:10.1029/2006JC003479.

Kobashi, F., H., S.-P. Xie, N. Iwasaka, and T. Sakamoto, 2008: Deep atmospheric response to the North Pacific oceanic subtropical front in spring. *J. Clim.*, **21**, 5960–5975.

Kobashi, F. and A. Kubokawa, 2012: Review on North Pacific subtropical countercurrents and subtropical fronts: role of mode waters in ocean circulation and climate. *J. Oceanogr.*, **68**, 21–43, doi:10.1007/s10872-011-0083-7.

Koch-Larrouy, A., G. Madec, P. Bouruet-Aubertot, T. Gerkema, L. Bessières, and R. Molcard, 2007: On the transformation of Pacific water into Indonesian Throughflow water by internal tidal mixing. *Geophys. Res. Lett.*, **34**, L04604, doi:10.1029/2006GL028405.

Kubokawa, A., 1997: A two-level model of subtropical gyre and subtropical countercurrent. *J. Phys. Oceanogr.*, **53**, 231–244.

Kubokawa, A., 1999: Ventilated thermocline strongly affected by a deep mixed layer: a theory for subtropical countercurrent. *J. Phys. Oceanogr.*, **29**, 1314–1333.

Kubokawa, A. and T. Inui, 1999: Subtropical countercurrent in an idealized ocean GCM. *J. Phys. Oceanogr.*, **29**, 1303–1313.

Kubota, H., R. Shirooka, and J. I. Hamada, 2011: Interannual rainfall variability over the eastern maritime continent. *J. Meteorolo. Soc. Jpn.*, **89**, 111–122.

Kuo, Y.-C. and C. S. Chern, 2011: Numerical study on the interactions between a mesoscale eddy and a western boundary current. *J Oceanogr.*, **67**, 263–272.

Kurogi, M. and K. Akitomo, 2003: Stable paths of the Kuroshio south of Japan determined by the wind stress field. *J. Geophys. Res.*, **108**, 3332, doi:10.1029/2003JC001853.

——— and ———, 2006: Effects of stratification on the stable paths of the Kuroshio and on their variation. *Deep Sea Res. I*, **53**, 1564–1577.

Lebedev, K. V. and M. I. Yaremchuk, 2000: A diagnostic study of the Indonesian Throughflow. *J. Geophys. Res.*, **105**, 11,243–11,258.

Lee, T. *et al.*, 2010: Consistency and fidelity of Indonesian-throughflow total volume transport estimated by 14 ocean data assimilation products. *Dynam. Atmos. Oceans*, **50**, 201–223, doi:10.1016/j.dynatmoce.2009.12.004.

Li, L., W. D. Nowlin, and J. Su, 1998: Anticyclonic rings from the Kuroshio in the South China Sea. *Deep Sea Res. I*, **45**, 1469–1482.

Li, L. and T. Qu, 2006: Thermohaline circulation in the Deep South China Sea Basin as inferred from oxygen distributions. *J. Geophys. Res.*, **111**, C05017,

Liang, W. D., T. Y. Tang, Y. J. Yang, M. T. Ko, and W. S. Chuang, 2003: Upper-ocean currents around Taiwan. *Deep Sea Res., Part II*, **50**(6–7), 1085–1105.

Lie, H.-J., C.-H. Cho, J.-H. Lee, P. Niiler, and J.-H. Hu, 1998: Separation of the Kuroshio water and its penetration onto the continental shelf west of Kyushu. *J. Geophys. Res.*, **103**, 2963–2976.

Lindstrom, E., R. Lukas, R. Fine, E. Firing, S. Godfrey, G. Meyers, and M. Tsuchiya, 1987: The western Tropical Pacific Ocean circulation study. *Nature*, **330**, 533–537.

Liu, C.-T. and R.-J. Liu, 1988: The deep current in the Bashi Channel. *Acta Oceanogr. Taiwanica* **20**, 107–116.

Liu, Q. and L. Li, 2007: Baroclinic stability of oceanic Rossby wave in the North Pacific Subtropical Eastwards Countercurrent. *Chin. J. Geophys.*, **50**, 84–93.

Lukas, R., 1988: Interannual fluctuations of the Mindanao Current inferred from sea level. *J. Geophys. Res.*, **93**, 6744–6748.

Lukas, R. and E. Lindstrom, 1991: The mixed layer of the western equatorial Pacific Ocean. *J. Geophys. Res.*, **96**, 3343–3357.

Lukas, R., E. Firing, P. Hacker, P. L. Richardson, C. A. Collins, R. Fine, and R. Gammon, 1991: Observations of the Mindanao Current during the Western Equatorial Pacific Ocean Circulation Study. *J. Geophys. Res.*, **96**, 7089–7104.

Lukas, R., T. Yamagata, and J. P. McCreary, 1996: Pacific low-latitude western boundary currents and the Indonesian throughflow. *J. Geophys. Res.*, **101**, 12209–12216.

Luther, D. S., D. E. Harrison, and R. A. Knox, 1983: Zonal winds in the central equatorial Pacific and El Niño. *Science*, **222**, 327–330

Maes, C., J. Picaut, and S. Belamari, 2005: Importance of the salinity barrier layer for the buildup of El Niño. *J. Clim.*, **18**, 104–118.

Masuda, A., 1982: An interpretation of the bimodal character of the stable Kuroshio path. *Deep Sea Res.*, **29**, 471–484.

Masuda, S., K. Akitomo, and T. Awaji, 1999: Effects of stratification and bottom topography on the Kuroshio path variation south of Japan. Part I: Dependence of path selection on velocity. *J. Phys. Oceanogr.*, **29**, 2419–2431.

Masuda, S. and K. Akitomo, 2000: Effects of stratification and bottom topography on the Kuroshio path variation south of Japan. Part II: Path transitions in a multiple equilibrium regime. *J. Phys. Oceanogr.*, **30**, 1431–1449.

Masumoto, Y. and T. Yamagata, 1991: Response of the western tropical Pacific to the Asian winter monsoon: the generation of the Mindanao Dome. *J. Phys. Oceanogr.*, **21**, 1386–1398.

Masumoto, Y. and T. Yamagata, 1996: Seasonal variations of the Indonesian Throughflow in a general ocean circulation model. *J. Geophys. Res.*, **110**, 12287–12293.

Masumoto, Y. *et al.*, 2004: A fifty-year eddy-resolving simulation of the world ocean — preliminary outcomes of OFES (OGCM for the Earth Simulator). *J. Earth Simulator*, **1**, 35–56.

Masumoto, Y., M. Nagura, S.-P. Xie, P. N. Vinayachandran, T. Miyama, Z. Yu, J. P. Mccreary, Jr, R. R. Hood and H. Gildor, 2015: Ocean Processes Relevant to Climate Variations in the Indian Sector. Ch. 2, World Scientific Series on Asia-Pacific Weather and Climate, Vol. 7 (this volume) Ed. S. Behera, T. Yamagata.

Matsuno,T., J.-S. Lee, and S. Yanao, 2009: The Kuroshio exchange with the South and East China Seas. *Ocean Sci.*, **5**, 303–312.

McBride, J. L., M. R. Haylock, and N. Nichols, 2003: Relationships between the Maritime Continent heat source and the El Niño–Southern Oscillation phenomenon. *J. Clim.*, **16**, 2905–2914.

McPhaden, M. J., H. P. Freitag, S. P. Hayes, B. A. Taft, Z. Chen, and K. Wyrtki, 1988: The response of the equatorial Pacific Ocean to a westerly wind burst in May 1986. *J. Geophys. Res.*, **93**, 10589–10603.

Metzger, E. J. and H. E. Hurlburt, 1996: Coupled dynamics of the South China Sea, the Sulu Sea, and the Pacific Ocean. *J. Geophys. Res.*, **101**, 12,331–12,352.

Metzger, E. J. and H. E. Hurlburt, 2001. The non-deterministic nature of Kuroshio penetration and eddy shedding in the South China Sea. *J. Phys. Oceanogr.*, **31**, 1712–1732.

Metzger, E. J., H. E. Hurlburt, X. Xu, J. F. Shriver, A. L. Gordon, J. Sprintall, R. D. Susanto, and H. M. van Aken, 2010: Simulated and observed circulation in the Indonesian Seas: 1/12o global HYCOM and the INSTANT observations. *Dynam. Atmos. Oceans*, **50**, 275–300, doi:10.1016/j.dynatmoce.2010.04.002.

Meyers, G., 1996: Variation of Indonesian Throughflow and the El Nino–Southern Oscillation. *J. Geophys. Res.*, **101**, 12,255–12,263.

Minobe, S, B. Qiu, M. Nonaka and H. Nakamura, 2015: Air-Sea Interaction Over the Western Boundary Currents in the Western North Pacific. Ch. 7, World Scientific Series on Asia-Pacific Weather and Climate, Vol. 7 (this volume) Ed. S. Behera, T. Yamagata.

Mitsudera, H. and R. Grimshaw, 1994: Capture and resonant forcing of solitary waves by the interaction of a baroclinic current with topography. *J. Phys. Oceanogr.*, **24**, 2217–2244.

Mitsudera, H., B. Taguchi, T.Waseda, and Y. Yoshikawa, 2006: Blocking of the Kuroshio large meander by baroclinic interaction with the Izu Ridge. *J. Phys. Oceanogr.*, **36**, 2042–2059.

Miyazawa, Y., X. Guo, and T. Yamagata, 2004: Roles of meso-scale eddies in the Kuroshio paths, *J. Phys. Oceanogr.*, **34**, 2203–2222.

Miyazawa, Y., S. Yamane, X. Guo, and T. Yamagata, 2005: Ensemble forecast of the Kuroshio meandering. *J. Geophys. Res.*, **110**, C10026, doi:10.1029/2004JC002426.

Miyazawa, Y., T. Kagimoto, X. Guo, and H. Sakuma, 2008: The Kuroshio large meander formation in 2004 analyzed by an eddy-resolving ocean forecast system. *J. Geophys. Res.*, **113**, C10015, doi:10.1029/2007JC004226.

Nakamura, H., H. Ichikawa, A. Nishina, and H.-J. Lie, 2003: Kuroshio path meander between the continental slope and the Tokara Strait in the East China Sea. *J. Geophys. Res.*, **108**(C11), 3360, doi:10.1029/2002JC001450.

Nakamura, H., 2005: Numerical study on the Kuroshio path states in the northern Okinawa Trough of the East China Sea. *J. Geophys. Res.*, **110**, C04003, doi:10.1029/2004JC002656.

Nakamura, H., T. Yamashiro, A. Nishina, and H. Ichikawa, 2006: Time–frequency variability of Kuroshio meanders in Tokara Strait. *Geophys Res. Lett.*, **33** L21605, doi:10.1029/2006GL027516.

H. Nakamura, A. Nishina, H. Ichikawa, M. Nonaka, and S. Sasaki, 2008: Deep countercurrent beneath the Kuroshio in the Okinawa Trough. *J. Geophys. Res.*, **113**, C06030, doi: 10.1029/2007JC004574.

Nakamura, H., A. Nishina, K. Tabata, M. Higashi, A. Habano, and T. Yamashiro, 2012: Surface velocity time series derived from satellite altimetry data in a section across the Kuroshio southwest of Kyushu. *J. Oceanogr.*, **68**, 321–336.

Nakamura, H., A. Nishina, and S. Minobe, 2012: Response of storm tracks to bimodal Kuroshio path states south of Japan. *J. Clim.*, **25**, 7772–7779.

Neale, R. B. and J. M. Slingo, 2003: The Maritime Continent and its role in the global climate: a GCM study. *J. Clim.*, **16**, 834–848.

Nitani, H., 1972. Beginning of the Kuroshio. Kuroshio: Its Physical Aspects of the Japan Current, University of Washington Press, Seattle, Washington. eds. H. Stommel and K. Yoshida, 129–163.

Nonaka, M. and S.-P. Xie, 2003: Covariations of sea surface temperature and wind over the Kuroshio and its extension: evidence for ocean-to-atmosphere feedback. *J. Clim.*, **16**, 1404–1413.

Oberhuber, J. M., 1988: An atlas based on the "COADS" data set: the budgets of heat, buoyancy and turbulent kinetic energy at the surface of the global ocean. Rep. 15, Max-Planck-Institut. fur Meteorologie, Hamburg, Germany.

Potemra, J. T., 1999: Seasonal variations of Upper Ocean Transport from the Pacific to the Indian Ocean via Indonesian Straits. *J. Phys. Oceanogr.*, **29**, 2930–2944.

Potemra, J. T. and N. Schneider, 2007: Interannual variations of the Indonesian throughflow. *J. Geophys. Res.*, **112**, C05035, doi:10.1029/2006JC003808.

Pujiana, K., A. L. Gordon, and J. Sprintall, 2013: Intraseasonal Kelvin wave in Makassar Strait, doi:10.1002/jgrc.20069, in press.

Qiu, B. and N. Imasato, 1990: A numerical study on the formation of the Kuroshio counter current and the Kuroshio branch current in the East China Sea. *Cont. Shelf Res.*, **10**(2), 165–184.

Qiu, B., T. Toda, and N. Imasato, 1990: On Kuroshio front fluctuations in the East China Sea using satellite and *in situ* observational data. *J. Geophys. Res.*, **95**, 18,191–18,203.

Qiu, B., 1999: Seasonal eddy field modulation of the North Pacific Subtropical Countercurrent: TOPEX/Poseidon observations and theory. *J. Phys. Oceanogr.*, **29**, 2471–2486.

Qiu, B. and R. Lukas, 1996: Seasonal and interannual variability of the North Equatorial Current, the Mindanao Current, and the Kuroshio along the Pacific western boundary. *J. Geophys. Res.*, **101**, 12,315–12,330.

Qiu, B. and S. M. Chen, 2010: Interannual-to-decadal variability in the bifurcation of the North Equatorial Current off the Philippines. *J. Phys. Oceanogr.*, **40**, 2525–2538.

Qiu, D., T. Yang, and Z. Guo, 1984: A westward current in the northeastern part of the South China Sea. *Trop. Oceanol.*, **33**, 65–73 (in Chinese, with English abstract).

Qu, T., T. Kagimoto, and T. Yamagata, 1997: A subsurface countercurrent along the east coast of Luzon. *Deep Sea Res. I*, **44**, 413–423.

Qu, T., H. Mitsudera, and T. Yamagata, 1998: On the western boundary currents in the Philippines Sea. *J. Geophys. Res.*, **103**, 7537–7548.

Qu, T., H. Mitsudera, and T. Yamagata, 1999: A climatology of the circulation and water mass distribution near the Philippine coast. *J. Phys. Oceanogr.*, **29**, 1488–1505.

Qu, T., H. Mitsudera, and T. Yamagata, 2000: Intrusion of the North Pacific water into the South China Sea. *J. Geophys. Res.*, **105**, 6415–6424.

Qu, T., 2000: Upper layer circulation in the South China Sea. *J. Phys. Oceanogr.* **30**, 1450–1460.

Qu, T. and R. Lukas, 2003: The bifurcation latitude of the North Equatorial Current in the Pacific. *J. Phys. Oceanogr.*, **33**, 5–18.

Qu, T., Y. Y. Kim, M. Yaremchuk, T. Tozuka, A. Ishida, and T. Yamagata, 2004: Can Luzon Strait Transport play a role in conveying the impact of ENSO to the South China Sea? *J. Clim.*, **17**(18), 3643–3656.

Qu, T., Y. Du, G. Meyers, A. Ishida, and D. Wang, 2005a: Connecting the tropical Pacific with Indian Ocean through South China Sea. *Geophys. Res. Lett.*, **32**, L24609, doi:10.1029/2005GL024698.

Qu, T., J. Strachan, G. Meyers, and J. Slingo, 2005b: Sea surface temperature and its variability in the Indonesian region. *Oceanography*, **18**, 50–61.

Qu, T., Y. Du, and H. Sasaki, 2006a: South China Sea throughflow: a heat and freshwater conveyor. *Geophys. Res. Lett.*, **33**, L23617, doi:10.1029/2006GL028350.

Qu, T., G. Girton, and J. Whitehead, 2006b: Deepwater overflow through Luzon Strait. *J. Geophys. Res.*, **111**, C01002, doi:10.1029/2005JC003139.

Qu, T., J. Gan, A. Ishida, Y. Kashino, and T. Tozuka, 2008: Semiannual variation in the western tropical Pacific Ocean. *Geophys. Res. Lett.*, **35**, L16602, doi:10.1029/2008GL035058.

Qu, T., and. T. Y. Song, 2009: Mindoro Strait and Sibutu Passage transports estimated from satellite data. *Geophys. Res. Lett.*, **36**, L09601, doi:10.1029/2009GL037314.

Qu, T., T. Y. Song, and T. Yamagata, 2009: South China Sea throughflow: its dynamics, variability, and implication for climate. *Dynam. Atmos. Oceans*, **47**, 3–14.

Qu, T., T.-L. Chiang, C.-R. Wu, P. Dutrieux, and D. Hu, 2012: Mindanao Current/Undercurrent in an eddy-resolving GCM. *J. Geophys. Res.*, **117**, C06026, doi:10.1029/2011JC007838.

Quadfasel, D., H. Kudrass, and A. Frische, 1990: Deep-water renewal by turbidity currents in the Sulu Sea. *Nature*, **348**, 320–322.

Ramage, C. S., 1968: Role of a tropical "Maritime Continent" in the atmospheric circulation. *Mon. Wea. Rev.*, **96**, 365–370.

Robinson, A. R. and B. Taft, 1972: A numerical experiment for the path of the Kuroshio. *J. Mar. Res.*, **30**, 65–101.

Rudnick, D. L., S. Jan, L. Centurioni, C. M. Lee, R.-C. Lien, J. Wang, D.-K. Lee, R.-S. Tseng, Y. Y. Kim, and C.-S. Chern, 2011: Seasonal and mesoscale variability of the Kuroshio near its origin. *Oceanogr.*, **24**, 52–63.

Saji, N. H., B. N. Goswami, P. N. Vinayachandran, and T. Yamagata, 1999: A dipole mode in the tropical Indian Ocean. *Nature*, **401**, 360–363.

Saiki, T., 1982: Relation between the geostrophic flux of the Kuroshio in the Eastern China Sea and its large meanders in south of Japan. *Oceanogr. Mag.*, **32**, 11–18.

Santoso, A., W. Cai, M. H. England, and S. J. Phipps, 2011: The role of the Indonesian Throughflow on ENSO dynamics in a coupled climate model. *J. Clim.*, **24**, 585–601.

Schiller, A., J. S. Godfrey, P. C. McIntosh, G. Meyers, and S. E. Wijffels, 1998: Seasonal near-surface dynamics and thermodynamics of the Indian Ocean and Indonesian Throughflow in a global ocean general circulation model. *J. Phys. Oceanogr.*, **28**, 2288–2312, doi:10.1175/1520-0485(1998)028<2288:SNSDAT>2.0.CO;2.

Schneider, N., 1998: The Indonesian Throughflow and the global climate system. *J. Clim.*, **11**, 676–689.

Sekine, Y., 1990: A numerical experiment on the path dynamics of the Kuroshio with reference to the formation of the large meander path south of Japan. *Deep Sea. Res.*, **37**, 359–380.

Shinoda, T., W. Han, E. J. Metzger, and H. E. Hurlburt, 2012: Seasonal variation of the Indonesian Throughflow in Makassar Strait. *J. Phys. Oceanogr.*, **42**, 1099–1123.

Shiraishi, S., S. Tsubaki, T. Shiga, S. Yamamoto, and D. Ueno, 1999: Long-term variability of the oceanographic conditions along a fixed hydrographic line (G-PN line) crossing the Kuroshio in the East China Sea. *Wea. Serv. Bull.*, **66**, S43–S49.

Shaw, P.-T., 1989: The intrusion of water masses into the sea southwest of Taiwan. *J. Geophys. Res.*, **94**, 18,213–18,226.

Shaw, P.-T., 1991: Seasonal variation of the intrusion of the Philippine sea water into the South China Sea. *J. Geophys. Res.*, **96**, 821–827.

Shaw, P.-T. and S.-Y. Chao, 1994: Surface circulation in the South China Sea. *Deep Sea Res. I.*, **41**, 1663–1683.

Sheremet, V., 2001: Hysteresis of a western boundary current leaping across a gap. *J. Phys. Oceanogr.*, **31**, 1247–1259.

Song, Y. T., 2006: Estimation of interbasin transport using ocean bottom pressure: theory and model for Asian marginal seas. *J. Geophys. Res.*, **111**, C11S19, doi:10.1029/2005JC003189.

Spall, M. A. and J. Pedlosky, 2005: Reflection and transmission of equatorial Rossby waves. *J. Phys. Oceanogr.*, **35**, 363–373.

Sprintall, J. and M. Tomczak, 1992: Evidence of the barrier layer in the surface layer of the tropics. *J. Geophys. Res.*, **97**, 7305–7316.

Sprintall, J., *et al.*, 2004: INSTANT: a new international array to measure the Indonesian Throughflow. *EOS*, **85**(39), 369.

Sprintall, J. and W. T. Liu, 2005: Ekman mass and heat transport in the Indonesian Seas. *Oceanography*, **18**(4), 88–97.

Sprintall, J., S. E. Wijffels, R. Molcard, and I. Jaya, 2009: Direct estimates of the Indonesian Throughflow entering the Indian Ocean: 2004–2006. *J. Geophys. Res.*, **114**, C07001, doi:10.1029/2008JC005257.

Sprintall, J., A. L. Gordon, P. Flament, and C. L. Villanoy, 2012: Observations of exchange between the South China Sea and the Sulu Sea. *J. Geophys. Res.*, **117**, C05036, doi:10.1029/2011JC007610.

Suarez, M. J. and P. S. Schopf, 1988: A delayed action oscillator for ENSO. *J. Atmos. Sci.*, **45**, 3283–3287.

Sugimoto, Y., S. Kimura, and K. Miyaji, 1988: Meander of the Kuroshio front and current variability in the East China Sea. *J. Oceanogr. Soc. Jpn.*, **44**, 125–135.

Sugimoto, S. and K. Hanawa, 2012: Relationship between the path of the Kuroshio in the south of Japan and the path of the Kuroshio Extension in the east. *J. Oceanogr.*, **68**, 219–225.

Sun, X.-P. and Y.-F. Su, 1994: On the variation of Kuroshio in East China Sea. *Oceanology of China Seas*, Vol. 1, Kluwer Academic, eds. D. Zhou, Y.-B. Liang, and C. K. Tseng, 49–58.

Susanto, R. D. and A. L. Gordon, 2005: Velocity and transport of the Makassar Strait throughflow. *J. Geophys. Res.*, **110**, C01005, doi:10.1029/2004JC002425.

Suzuki, T., T. T. Sakamoto, T. Nishimura, N. Okada, S. Emori, A. Oka, and H. Hasumi, 2005: Seasonal cycle of the Mindanao Dome in the CCSR/NIES/FRCGC atmosphere–ocean coupled model. *Geophys. Res. Lett.*, **32**, L17604, doi:10.1029/2005GL023666.

Takahashi, D., Guo, X., Morimoto, A., and Kojima, S. 2009: Biweekly periodic variation of the Kuroshio axis northeast of Taiwan as revealed by ocean high-frequency radar. *Conti. Shelf Res.*, **29**, 1896–1907.

Talley, L. D. and J. Sprintall, 2005: Deep expression of the Indonesian Throughflow: Indonesian Intermediate Water in the South Equatorial Current. *J. Geophys. Res.*, **110**, C10009, doi:10.1029/2004JC002826.

Tang, T. Y. and Y. J. Yang, 1993: Low frequency current variability on the shelf break northeast of Taiwan. *J. Oceanogr.*, **49**, 193–210.

Tang, T. Y., Y. Hsueh, Y. J. Yang, and J. C. Ma, 1999: Continental slope flow northeast of Taiwan. *J. Phys. Oceanogr.*, **29**, 1353–1362.

Tang, T. Y., J. H. Tai, and Y. J. Yang, 2000: The flow pattern north of Taiwan and the migration of the Kuroshio. *Cont. Shelf Res.*, **20**, 349–371.

Tessler, Z. D., A. L. Gordon, L. J. Pratt, and J. Sprintall, 2010: Transport and dynamics of the Panay Sill overflow in the Philippine Seas. *J. Phys. Oceanogr.*, **40**, 2679–2695.

Tian, J., Q. Yang, X. Liang, D. Hu, F. Wang, and T. Qu, 2006: The observation of Luzon Strait transport. *Geophys. Res. Lett.*, **33**, L19607, doi:10.1029/2006GL026272.

Tian, J., Q. Yang, and W. Zhao, 2009: Enhanced diapycnal mixing in the South China Sea. *J. Phys. Oceanogr.*, **39**, 3191–3203, doi:10.1175/2009JPO3899.1.

Toole, J. M., R. C. Millard, Z. Wang, and S. Pu, 1990: Observations of the Pacific North Equatorial Current bifurcation at the Philippine coast. *J. Phys. Oceanogr.*, **20**, 307–318.

Tozuka, T., T. Kagimoto, Y. Masumoto, and T. Yamagata, 2002: Simulated multiscale variations in the western tropical Pacific: the Mindanao Dome revisited. *J. Phys. Oceanogr.*, **32**, 1338–1359.

Tozuka, T. and T. Yamagata, 2003: Annual ENSO. *J. Phys. Oceanogr.*, **33**, 1338–1359.

Tozuka, T., J.-J. Luo, S. Masson, S. K. Behera, and T. Yamagata, 2005: Annual ENSO simulated in a coupled ocean–atmosphere model. *Dynam. Atmos. Oceans*, **39**, 41–60.

Tozuka, T., J. J. Luo, S. Masson, and T. Yamagata, 2007a: Seasonally stratified analysis of simulated ENSO thermodynamics. *J. Clim.*, **20**, 4615–4627.

Tozuka, T., T. Qu, and T. Yamagata, 2007b: Effect of South China Sea throughflow on the Makassar Strait throughflow. *Res. Lett.*, **34**, L12612, doi:10.1029/2007GL030420.

Tozuka, T., T. Qu, and T. Yamagata, 2009: Impacts of the South China Sea throughflow on seasonal and interannual variations of the Indonesian throughflow. *Dynam. Atmos. Oceans*, **47**, 73–85.

Tsujino, H., N. Usui, and H. Nakano, 2006: Dynamics of Kuroshio path variations in a high-resolution general circulation model. *J. Geophys. Res.*, **111**, C11001, doi:10.1029/2005JC003118.

Tsukamoto, K., 1992: Discovery of the spawning area for Japanese eel. *Nature*, **356**, 789–791.

Uda, M. and K. Hasunuma, 1969: The eastward subtropical countercurrent in the western North Pacific Ocean. *J. Oceanogr. Soc. Jpn.*, **25**, 201–210.

Ueki, I., Y. Kashino, and Y. Kuroda, 2003: Observation of current variations off the New Guinea coast including the 1997–1998 El Niño period and their relationship with Sverdrup transport. *J. Geophys. Res.*, **108**, 3243, doi:10.1029/2002JC001611.

Ueki, I., 2011: Evidence of wind–evaporation–sea surface temperature (WES) feedback in the western Pacific warm pool during the mature phase of the 1997–98 El Niño. *Geophys. Res. Lett.*, **38**, L11603, doi:10.1029/2011GL047179.

Usui, N., H. Tsujino, Y. Fujii, and M. Kamachi, 2008a: Generation of a trigger meander for the 2004 Kuroshio large meander. *J. Geophys. Res.*, **113**, C01012, doi:10.1029/2007JC004266.

Usui, N., H. Tsujino, H. Nakano, and Y. Fujii, 2008b: Formation process of the Kuroshio large meander in 2004. *J. Geophys. Res.*, **113**, C08047, doi:10.1029/2007JC004675.

Usui, N., H. Tsujino, H. Nakano, Y. Fujii, and M. Kamachi, 2011: Decay mechanism of the 2004/05 Kuroshio large meander, *J. Geophys. Res.*, **116**, C10010, doi:10.1029/2011JC007009.

van Aken, H. M., 2005: Dutch oceanographic research in Indonesia in colonial times. *Oceanography*, **18**(4), 30–41.

Vranes, K., A. L. Gordon, and A. Ffield, 2002: The heat transport of the Indonesian throughflow and implications for the Indian Ocean heat budget. *Deep Sea Res.*, **40**.

Wang, B., F. Huang, Z. Wu, J. Yang, X. Fu, and K. Kikuchi, 2009: Multi-scale climate variability of the South China Sea monsoon: a review. *Dynam. Atmos. Oceans*, **47**(1–3), 15–37.

Wang, C., 2001: A unified oscillator model for the El Niño–Southern Oscillation. *J. Clim.*, **14**, 98–115.

Wang, D., Q. Liu, R. Huang, Y. Du, and T. Qu, 2006: Interannual variability of the South China Sea throughflow inferred from wind data and an ocean data assimilation product. *Geophys. Res. Lett.*, **33**, L14605, doi:10.1029/2006GL026316.

Wang, F. and D. Hu, 2010: Introduction to international NPOCE program. *Chin. J. Oceanol. Limnol.*, **28**, 953–953.

Wang, G., S.-P. Xie, T. Qu, and R. Huang, 2011: . Deep South China Sea Circulation. *Geophys. Res. Lett.*, **38**, L05601, doi:10.1029/2010GL046626.

Wang, J., 1986: Observation of abyssal flows in the Northern South China Sea. *Acta Oceanogr. Taiwanica*, **16**, 36–45.

Wang, Q. and D. Hu, 2006: Bifurcation of the North Equatorial Current derived from altimetry in the Pacific Ocean. *J. Hydrodynam.*, **18**, 620–626.

Weisberg, R. H. and C. Wang, 1997: A western Pacific oscillator paradigm for the El Niño–Southern Oscillation. *Geophys. Res. Lett.*, **24**, 779–782.

White, W. B. and J. P. McCreary, 1976: On the formation of the Kuroshio meander and its relationship to the large-scale ocean circulation. *Deep Sea Res.*, **23**, 33–47.

White, W. B., K. Hasunuma, and H. Solomon, 1978: Large-scale seasonal and secular variability of the subtropical front in the western North Pacific from 1954 to 1974. *J. Geophys. Res.*, **83**, 4531–4544.

Wijffels, S., E. Firing, and J. Toole, 1995: The mean structure and variability of the Mindanao Current at 8°N. *J. Geophys. Res.*, **100**, 18,421–18,435.

Wijffels, S. and G. Meyers, 2003: An intersection of oceanic waveguides: variabiliy in the Indonesian Throughflow region. *J. Phys. Oceanogr.*, **34**, 1232–1253.

Worthington, V. L. and H. Kawai, 1972: Comparison between deep sections across the Kuroshio and the Florida Current and Gulf Stream. *Kuroshio, Its Physical Aspects.* Washington University Press, eds. H. Stommel and K. Yoshida, 371–385.

Wu, C.-R., P.-T. Shaw, and S.-Y. Chao, 1998: Seasonal and interannual variation of the velocity field of the South China Sea. *J. Oceanogr.*, **54**, 361–372.

Wu, C.-R. and C.-W. J. Chang, 2005: Interannual variability of the South China Sea in a data assimilation model. *Geophys. Res. Lett.*, **32**, L17611, doi:10.1029/2005GL023798.

Wu C.-R. and T.-L. Chiang, 2007: Mesoscale eddies in the northern South China Sea. *Deep Sea Res. II*, **54**, 1575–1588.

Wyrtki, K., 1961: Physical oceanography of the southeast Asian waters. Naga Report 2, Scripps Institution of Oceanography, La Jolla, California.

Wyrtki, K., 1985: Water displacements in the Pacific and the genesis of El Niño cycles. *J. Geophys. Res.*, **90**, 7129–7132.

Xie, S.-P., C. Deser, G.A. Vecchi, J. Ma, H. Teng, and A. T. Wittenberg, 2010: Global warming pattern formation: sea surface temperature and rainfall. *J. Clim.*, **23**, 966–986.

Xie, S.-P., L. Xu, Q. Liu, and F. Kobashi, 2011: Dynamical role of mode Water ventilation in decadal variability in the central subtropical gyre of the North Pacific. *J. Clim.*, **24**, 1212–1225.

Xie, P. and P. A. Arkin, 1997: Global precipitation: a 17-year monthly analysis based on gauge observations, satellite estimates, and numerical model outputs. *Bull. Am. Meteorol. Soc.*, **78**, 2539–2558.

Xu, L. X., S.-P. Xie, Q. Liu, and F. Kobashi, 2012a: Response of the North Pacific Subtropical Countercurrent and its variability to global warming. *J. Oceanogr.*, **68**, 127–137, doi:10.1007/s10872-011-0031-6.

Xu, L., S.-P. Xie, and Q. Liu, 2012b: Mode water ventilation and Subtropical Countercurrent over the North Pacific in CMIP5 simulations and future projections. *J. Geophys. Res.-Oceans*, **117**, C12009, doi:10.1029/2012JC008377.

Xue, H., F. Chai, N. Pettigrew, D. Xu, M. Shi, and J. Xu, 2004. Kuroshio intrusion and the circulation in the South China Sea. *J. Geophys. Res.*, **109**, C02017, doi:10.1029/2002JC001724.

Yamagata, T. and S. Umatani, 1987: The capture of current meander by coastal geometry with possible application to the Kuroshio current. *Tellus*, **39A**, 161–169.

Yamagata, T., Y. Morioka and S. Behera, 2015: Old and new faces of climate variations, Ch. 1, World Scientific Series on Asia-Pacific Weather and Climate, Vol. 7 (this volume), eds. S. Behera, T. Yamagata.

Yamanaka, G., H. Ishizaki, M. Hirabara, and I. Ishikawa, 2008: Decadal variability of the Subtropical Front of the western North Pacific in an eddy-resolving ocean general circulation model.

J. Geophys. Res., **113**, C12027, doi:10.1029/2008JC005002.

Yang, D., B. Yin, Z. Liu, and X. Feng, 2011: Numerical study of the ocean circulation on the East China Sea shelf and a Kuroshio bottom branch northeast of Taiwan in summer. *J. Geophys. Res.*, **116**, C05015, doi:10.1029/2010JC006777.

Yang, D., B. Yin, Z. Liu, T. Bai, J. Qi, and H. Chen, 2012: Numerical study on the pattern and origins of Kuroshio branches in the bottom water of southern East China Sea in summer. *J. Geophys. Res.*, **117**, C02014, doi:10.1029/2011JC007528.

Yang, Y., C.-T. Liu, J.-H. Hu, and M. Koga, 1999: Taiwan Current (Kuroshio) and impinging eddies. *J. Oceanogr.*, **55**, 609–617.

Yaremchuk, M. and T. Qu, 2004: Seasonal variability of the circulation near the Philippine coast. *J. Phys. Oceanogr.*, **34**, 844–855.

Yasuda, I., J.-H. Yoon, and N. Suginohara, 1985: Dynamics of the Kuroshio large meander — barotropic model. *J. Oceanogr. Soc. Jpn.*, **41**, 259–273.

Yoon, J.-H. and I. Yasuda, 1987: Dynamics of the Kuroshio large meander: two-layer model. *J. Phys. Oceanogr.*, **17**, 66–81.

Yoshida, K. and T. Kidokoro, 1967: A subtropical countercurrent in the North Pacific — an eastward flow near the Subtropical Convergence. *J. Oceanogr. Soc. Jpn.*, **23**, 88–91.

Yu, K. and T. Qu, 2013: Imprint of the Pacific Decadal Oscillation on the South China Sea throughflow variability. *J. Clim.* (under review).

Yu, L. and R. A. Weller, 2007: Objectively analyzed air–sea heat fluxes for the global ice-free oceans (1981–2005). *Bull. Am. Meteorol. Soc.*, **88**, 527–539.

Yu, L., R. A. Weller, and W. T. Liu, 2003: Case analysis of a role of ENSO in regulating the generation of westerly wind bursts in the western equatorial Pacific. *J. Geophys. Res.*, **108**, 3128, doi:10.1029/2002JC001498.

Yu, Z., S. Shen, J. P. McCreary, M. Yaremchuk, and R. Furue, 2007: South China Sea Throughflow as evidenced by satellite images and numerical experiments. *Geophys. Res. Lett.*, **34**, L01601, doi:10.1029/2006GL028103.

Yuan, D., M. M. Rienecker, and P. S. Schopf, 2004: Long wave dynamics of the interannual variability in a numerical hindcast of the equatorial Pacific Ocean circulation during the 1990s. *J. Geophys. Res.*, **109**, C05019, doi:10.1029/2003JC001936.

Yuan, D., W. Han, and D. Hu, 2006: Surface Kuroshio path in the Luzon Strait area derived from satellite remote sensing data. *J. Geophys. Res.*, **111**, C11007, doi:10.1029/2005JC003412.

Yuan, Y., A. Kaneko, J. Su, X. Zhu, Y. Liu, N. Gohda, and H. Chen, 1998: The Kuroshio east of Taiwan and in the East China Sea and the currents east of Ryukyu Islands during early summer of 1996. *J. Oceanogr.*, **54**, 217–226.

Yuan, Y., G. Liao, and X. Xu, 2007: Three-dimensional diagnostic modeling study of the South China Sea circulation before onset of summer monsoon 1998. *J. Oceanogr.*, **63**, 77–100.

Zhang, D. X., T. N. Lee, W. E. Johns, C. T. Liu, and R. Zantopp, 2001: The Kuroshio east of Taiwan: modes of variability and relationship to interior ocean mesoscale eddies. *J. Phys. Oceanogr.*, **31**(4), 1054–1074.

Zhao, L. and X. Guo, 2011: Influence of cross-shelf water transport on nutrients and phytoplankton in the East China Sea: a model study. *Ocean Sci.*, **7**, 27–43, doi:10.5194/os-7-27-2011.

Zhou, C., W. Zhao, J. Tian, Q. Yang, and T. Qu, 2014: Variability of the Deep Water Overflow in the Luzon Strait. *J. Phys. Oceanogr.*, **44**(11), 2972–2986, doi:10.1175/JPO-D-14-0113.1?af=R.

Zhu, X.-H., I.-S. Han, J.-H. Park, H. Ichikawa, K. Murakami, A. Kaneko, and A. Ostrovskii, 2003: The northeastward current southeast of Okinawa Island observed during November 2000 to August 2001. *Geophys. Res. Lett.*, **30**(2), 1071, doi:10.1029/2002GL015867.

Zhu, X.-H., H. Ichikawa, K. Ichikawa, and K. Takeuchi, 2004: Volume transport variability southeast of Okinawa Island estimated from satellite altimeter data. *J. Oceanogr.*, **60**, 953–962.